Evolving Earth 3 (2025) 100059

Contents lists available at ScienceDirect

Evolving Earth

journal homepage: www.sciencedirect.com/journal/evolving-earth

Genesis, classification, tectonic setting and economic potential of global granitic pegmatites: A review

P.L. Dharmapriya [a,*], D.W.M. Disanayaka [a], H.M.T.G.A. Pitawala [a,b], Sanjeewa P.K. Malaviarachchi [a], N.D. Subasinghe [c]

[a] Department of Geology, Faculty of Science, University of Peradeniya, 20400, Sri Lanka
[b] Postgraduate Institute of Science, University of Peradeniya, 20400, Sri Lanka
[c] National Institute of Fundamental Studies, Hantana Road, Kandy, 20000, Sri Lanka

ARTICLE INFO

Keywords:
Granitic pegmatites
Pegmatite classification
Industrial minerals
Strategic metals
Coloured gemstones

ABSTRACT

Granitic pegmatites have attracted a significant interest of petrologists and mineralogists due to their complex genetic characteristics and substantial economic value. Although numerous reviews addressed specific aspects such as genesis, classification, economic potential, and tectonic setting, a comprehensive review integrating all these facets in a single article has been lacking. This study fills that gap by offering a holistic review that synthesizes these key dimensions. It examines prevailing theories on pegmatite genesis, traces the evolution of classification systems, and assesses the economic importance of pegmatites as sources of industrial minerals, strategic metals, and gemstones, as well as their association with different tectonic settings.

The crystallization of the majority of granitic pegmatites is widely acknowledged to occur in the presence of a viscous, volatile-rich polymerized silicate magma, concomitant with supercritical aqueous fluids. Consequently, granitic pegmatites can frequently be conceded as a hybrid rock derived through igneous and hydrothermal processes. Various criteria, such as the emplacement depth of granitic pegmatites, their association with metamorphism and granitic plutons, geochemical signatures, and their relationships with host rocks, have traditionally been employed for the classification of granitic pegmatites. However, none of the classifications has been accepted unequivocally.

Pegmatitic melt is often rich in chemical constituents (including volatiles) that are incompatible in common rock-forming minerals. In addition to rare earth elements, pegmatites are commonly enriched in rare elements such as Li, B, Be, Cs, and Ta. Because they are incompatible in common rock-forming minerals, these elements tend to create specific mineral phases that can host themselves. As a result, the concentration of trace elements such as Li, B, Cs, Ta, and Bi in these bodies are enriched to levels as high as a thousand times higher than the typical crustal abundance.

Granitic pegmatites encompass a diverse array of economic commodities, serving as repositories for industrial minerals and sources for strategic metals like Ta, Cs, Sn, Nb, Be, Sb, W, Co, and rare earth elements. Furthermore, they contribute as reservoirs of fluxing components, including Li, P, F, and B, while serving as sources of precious and semi-precious gemstones and some radioactive minerals. The global distribution of pegmatite ages suggests a linkage between the age of pegmatite formation and supercontinent assembly. The Li, Ce and Ta enriched (LCT) granitic pegmatites form part of the orogenic suites associated with crustal shortening in zones of subduction and instances of continental collision. The Nb, Y, and F-enriched (NYF) pegmatites are mainly interpreted as products of anorogenic suites and formed mainly in extensional settings.

1. Introduction

Pegmatites are igneous rocks characterized by a granitic composition and are distinguished from other igneous formations by their exceptionally coarse yet variable grain size or by an abundance of crystals exhibiting skeletal, graphic, or other strongly directional growth habits (London, 2008). While there is a prevailing consensus among petrologists regarding the spectrum from magmatic to

---

* Corresponding author. Department of Geology, Faculty of Science, University of Peradeniya, Sri Lanka.
E-mail address: prasannad@sci.pdn.ac.lk (P.L. Dharmapriya).

https://doi.org/10.1016/j.eve.2025.100059
Received 11 May 2024; Received in revised form 29 December 2024; Accepted 10 January 2025

magmatic-hydrothermal processes as the likely genesis of pegmatites (e.g., Hunt, 1871; Landes, 1937; Ramberg, 1952; Reitan, 1965; Roedder, 1981; Chiarenzelli et al., 2019; Xu et al., 2024), the complete understanding of their origin remains elusive. The historical definitions of pegmatites, as outlined in Table 1, reveal a progression from simple descriptive terms based on grain size and mineral composition to more complex and nuanced understandings that consider textural variability and growth habits.

Pegmatite occurrences, typically ranging from a few cm-to m-scale, can extend impressively to several Km^2 (e.g., London and Kontak, 2012; Dharmapriya et al., 2021; Li et al., 2023). These formations are ubiquitously distributed across continents, found both within ancient cratons and younger, marginal mountain belts (London, 2018; Jain et al., 2020; Wang et al., 2023). Composed of interlocking large crystals of varying sizes, pegmatites commonly host crystals exceeding 2.5 cm, with remarkable instances of crystals surpassing 10 m in length reported (Kozłowski and Sachanbiński, 2007; London and Kontak, 2012). Occasionally, these crystals exhibit systematic dispersion from the margins to the centres of the bodies, showcasing distinctive mineralogical zonation (London, 2014). Pegmatites are primarily granitic in composition, with quartz, feldspar, and mica as their main mineral constituents, making them a significant source of these minerals (Dill, 2015; London, 2015).

Granitic pegmatites have been a focal point of research among petrologists and mineralogists due to their profound economic significance. These formations serve as storehouses for essential industrial minerals, including quartz, feldspars and micas (Roedder, 1992; Glover et al., 2012; Kesler et al., 2012; London and Morgan, 2012; Dill, 2015; Cardoso-Fernandes et al., 2023). Furthermore, certain pegmatites exhibit rare earth element concentrations that are thousand times higher than crustal abundance, establishing granitic pegmatites as a noteworthy source for strategic metal-bearing minerals (Černý, 1991a; Simmons and Webber, 2008; Linnen et al., 2012; Bradley et al., 2017; Feng et al., 2023). Pegmatites also host precious and semiprecious gemstones (Simmons, 2007; Simmons et al., 2012; McManus et al., 2008; Beurlen et al., 2013; Hussain et al., 2021; Mauthner, 2024). Additionally, pegmatites may contain fluxing components and energy minerals, further augmenting their geological importance (London and Kontak, 2012; Dill, 2015; London, 2018). Distinct from typical igneous rocks, pegmatites deviate due to their enigmatic origin as well as their unique mineralogy and textures.

Table 1
Selected examples of the definition of “pegmatite” through history.

Publication	Definition
Bastin (1911) (Geology report)	*“The granite-pegmatites, in which are. found feldspar, quartz, mica, and gem minerals, are composed of the same mineral constituents as the ordinary granites of the State, and differ from these principally in their greater coarseness and in their very uneven texture.”*
Landes (1933) (Original research article)	The word ’pegmatite" was coined originally by Haüy in the early years of the 19th century as a descriptive term applied to rocks with a graphictexture. In 1849 ″pegmatite" was used by Delesse (Williams,1885) to designate a very coarse granite and gradually the use of the term was extended to include all types of exceptionally coarse plutonic rocks whether graphic or not.
Jahns (1953) (Research article)	“The term pegmatite is applied by geologists mainly to those intrusive igneous rocks that are holocrystalline and at least in part very coarse-grained. Marked irregularities in grain size are characteristic, and in some masses of pegmatite, the coarsest crystals are enormous.”
Gillespie and Styles (1999) (a rock classification scheme)	*“The term pegmatite should be used only for veins comprised of coarse or very coarse crystals. Such rocks should be named by listing the component minerals as qualifiers in front of the term pegmatite, for example biotite-quartz-feldspar pegmatite.”*
Best (2003) (Textbook)	*“Pegmatite: Rocks of highly variable grain size in which individual crystals can be as much as several m. Usually refers to a textural variety of leucocratic granite.”*
London (2008) (Textbook)	*“Pegmatites are essentially igneous rock, mostly of granitic composition, that is distinguished from other igneous rocks by its extremely coarse but variable grain size, or by an abundance of crystals with skeletal, graphic, or other strongly directional growth habits.”*
London et al. (2012) (Review article)	*“Pegmatites are texturally distinct variants of the more common and more voluminous plutonic igneous rocks, including gabbros, granites, syenites, etc. Whereas common plutonic bodies tend to be mineralogically and texturally homogeneous throughout large volumes of rock, pegmatites are precisely the opposite. Exceedingly coarse crystal size is a hallmark of pegmatites for most geoscientists but gigantic crystal size is not the sole or even a necessary defining factor.”*
Simmons et al. (2024) (Review article)	*“Pegmatites are among the most intriguing of all the igneous rock types. They form from the crystallization of an igneous melt and show very coarse-grained to gigantic-sized textures in intrusive igneous rocks, with crystals generally more than 2.5 cm”*

The genesis of pegmatites has undergone investigation for over a century, with various proposed mechanisms. However, achieving a universal consensus on the formation of pegmatites remains elusive (e.g., Niggli, 1920; Merritt, 1924; Schaller, 1925; Landes, 1933; Cameron et al., 1949; Jahns and Burnham, 1969; Simmons and Webber, 2008; W. B. Simmons et al., 2024). Meanwhile, over the last six decades, the diverse spectrum encompassing mineralogical, textural, geochemical, and economic characteristics, along with their relation to the host rock of granitic pegmatites, has been the subject of numerous attempts at classification (Ginsburg and Rodionov, 1960; Ginsburg et al., 1979; Černý, 1991a; Zagorsky et al., 1999; Wise, 1999; Pezzotta, 2001; Černý and Erict, 2005; Martin and De Vito, 2005; Fuchsloch et al., 2018; Beskin and Marin, 2018).

Numerous previous work on granitic pegmatites have been published, examining (a) their genesis, elucidating the characteristics of the source magma, such as geochemical constituents, cooling rates, and the formation of coarse-grained texture, as well as the pressure-temperature (*P-T*) conditions of crystallization (e.g. London, 2005; Simmons and Webber, 2008; London et al., 2012a; Černý et al., 2012), including discussions on heterogeneity and zonations (London, 2014); (b) classification schemes (Černý and Ercit, 2005; Simmons, 2005); (c) their economic potential as sources of industrial minerals (Glover et al., 2012), strategic metals (e.g., Linnen et al., 2012), and precious gemstones (e.g., Shigley et al., 1984; Simmons et al., 2012); and (d) the tectonic settings in which pegmatites are formed (Martin and De Vito, 2005). Nevertheless, these review articles have often focused singularly on specific aspects, and a comprehensive review covering all these dimensions is notably absent.

In this paper, we aim to provide a comprehensive historical overview, compiling knowledge on granitic pegmatites from early studies to the latest research. We place particular emphasis on (a) mineralogy and anatomy, exploring the genesis of pegmatitic melt, its chemical constituents, and crystallization conditions; (b) attempts at classifying granitic pegmatites; and (c) their economic potential, as well as (d) the tectonic settings in which pegmatites are formed. These multifaceted aspects have not been collectively reviewed by previous researchers, contributing to a more holistic understanding of granitic pegmatites.

2. Mineralogical and Anatomical features of granitic pegmatites

The granitic pegmatitic composition shares a simple mineral assemblage with granite, featuring dominant phases such as quartz, albite, and potassium feldspar—either orthoclase or microcline. Martin (1988) showed how the Al-Si ordering in K-feldspar does not follow a unique path and the K-feldspar, sanidine, orthoclase, and microcline are pseudomorphs of the magmatic phases. They have emphasized the discontinuous and continuous transformation of these phases during pegmatite formation. Muscovite and/or biotite ‘books’ commonly occur as minor mineral phases in many granitic pegmatites (London and

Kontak, 2012; Ndikumana et al., 2020). In addition, granitic pegmatites may bear over fifty accessory mineral species such as iron oxides, zircon, fluorite, apatite, lepidolite, amblygonite, spodumene, tourmaline with variable colours, beryl, amber-coloured topaz, and rose and amethystine quartz (Bastin, 1910; Abdelfadil et al., 2016; Chakraborty et al., 2024). Table 2 summarizes the occurrences of accessory minerals in some selected pegmatites in the globe. Minerals like sericite, epidote, and chlorite often occur as secondary phases (Abdelfadil et al., 2016; Georgieva et al., 2022).

The mineralogical composition as well as the elemental concentration in pegmatite is influenced by the distance of the pegmatite from the source (e.g., Simmons and Webber, 2008; Fredriksson, 2017). For instance, the Na/K ratio in feldspars correlates well with the source rock (Stugard, 1958; Tang et al., 2018). K-rich pegmatites are found closest to the source, while Na-rich pegmatites are situated at the most distal end of the pegmatite source (Černý et al., 2012). The K/Rb ratio decreases with the advancing crystallization of K-feldspar (Černý and Erict, 1985). These fractionation patterns play a significant role in determining the exotic mineralogy of the pegmatite body (Trueman and Černý, 1982; Breaks et al., 2005). Post-crystallization processes, for example, the subsolidus reaction of solids with aqueous fluids (primary or secondary) facilitate the formation of new mineral phases in granitic pegmatites (e.g., Černý, 1972). A detailed summary of the formation of industrial minerals, strategic metals, gemstones, and energy minerals is provided in Section 7.

Pegmatites can exhibit zonation or remain unzoned based on mineralogy and rock fabrics. Two types of zoned pegmatites can be recognized based on their scale: (i) regional zonation, where chemical complexity increases with distance from granitic or other thermal sources, and (ii) internal zonation (Fig. 1), representing mineralogical and textural changes within individual pegmatite bodies (London, 2014). Cameron et al. (1949) proposed the nomenclature and defined the patterns of internal zonation within granitic pegmatites that are in use today. The four main zones defined by these authors are (i) border (ii) wall (iii) intermediate and (iv) core (Fig. 1). As summarized by London (2014): (i) The border zone is a thin layer (mm to cm thick) that surrounds the pegmatite body in contact with its host rocks. The grain size is fine-grained (∼2–5 mm), and the texture is hypidiomorphic granular. (ii) The wall zone is a thick margin surrounding the pegmatite bodies, containing plagioclase and predominantly quartz, along with minerals such as muscovite, biotite, K-feldspar, garnet, tourmaline, apatite, primary chlorite, beryl, and columbite as accessory minerals (London, 2014; Pattison and DeBuhr, 2015). (iii) The intermediate zone is symmetrically or asymmetrically distributed through the pegmatite, carrying exceedingly coarse-grained and blocky textures. These textures result from the buildup of fluxing components in a boundary layer of liquid that advances into the pegmatite along the crystal growth front (Kesler et al., 2012). The zone contains perthitic microcline, plagioclase, muscovite, spodumene, and petalite with quartz. (iv) The core of a pegmatite constitutes its innermost unit within the zoned structure, characterized by a singular mass or multiple repetitions of the same mineralogy at the same structural or sequential position. In granitic pegmatites, monomineralic quartz cores are frequently encountered (London, 2014). Nevertheless, in certain pegmatites (Li-rich pegmatite), in addition to quartz, the latest primary units may occasionally exhibit a quartz-poor composition, featuring albite and lepidolite, along with various typically rare minerals. The proportions of core material to the other zones can be exceedingly variable, and monomineralic quartz cores predominate in granitic pegmatites (Brögger, 1890).

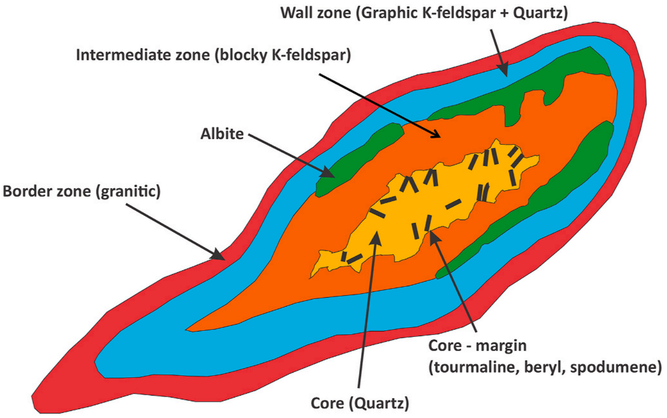

Fig. 1. Internal structure of zoned pegmatites in a schematic horizontal section (modified after Černý, 1991a).

Brögger (1890) proposed zonation as the simultaneous interaction of silicate melt and aqueous fluid, a concept subsequently widely described

Table 2
Occurrences of accessory minerals in some selected pegmatite/pegmatite fields in the world.

pegmatite/pegmatite field	Major mineral	Minor/Accessory minerals	Age (Ma)	References
The Tanco pegmatite at Bernic Lake, Manitoba, Canada	Albite, microcline, quartz, mica	Hafnium zircon, tantalite, lepidolite, pollucite, petalite, amblygonite	∼2631	Černý and Siivola (1980); Černý et al., (2005); Brown (2001); Camacho et al. (2012); Brown et al. (2017); London (2024);
Greenbushes, Western Australia	Albite, Spodumene, quartz, biotite,	Tourmaline, Ta-ilmenite, Ta-rutile, cassiterite, apatite	∼2530	Partington et al. (1995); Klementová and Rieder (2004); Phelps-Barber et al. (2022)
Wodgina, Western Australia	Albite, quartz, muscovite	Columbite, cassiterite, petalite, beryl, wodginite	∼2800	Tindle et al. (1998); Sweetapple and Collins (2002); Richter et al. (2014); Jacobson (2021)
Tochka deposit, Karagoin–Saryozek zone in East Kazakhstan	Microcline, albite, quartz	Zircon with disseminated U phase (uraninite), Rutile, Ni phase (bunsenite?), cassiterite, tantalite, columbite, native tin, pyrolusite	∼292	Zimanovskaya et al., 2022
Bikita, Zimbabwe	Quartz, albite, Mica	Tourmaline, zinnwaldite, garnet, tourmaline and epidote, beryl, petalite, tantalite, amblygonite	∼2600	Černý et al. (2003); Dittrich et al. (2019); Gogodo (2021); Chagondah et al. (2024)
Manono-Kitotolo, Democratic Republic of Congo	Quartz, muscovite, microcline and albite	Beryl, spodumene, columbite, tantalite, cassiterite, thoreaulite, wodginite and tapiolite, fluorite, zircon, thoreaulite, arsenopyrite, pyrite, ilmenite, autunite	∼930	Thoreau (1950); Bassot and Morio (1989); Melcher et al. (2008); Dewaele et al. (2016)
Alto Ligonha, Mozambique	Quartz, albite K-feldspar, muscovite	Zinnwaldite, lepidolite, polylithionite, beryl, garnet, tourmaline, cassiterite, gahnite, columbite, tantalite, rutile, some uranium minerals	∼480	Gomes et al. (2009); Neiva (2013); Cronwright (2014); Gomes and Neiva (2022); Altieri et al. (2024)
Mina Gerais, Brazil	Quartz, feldspar, mica	Tourmaline, aquamarine, topaz, beryl, bergslagite, herderite, lithiophosphate, lithiotantite, kosnarite	∼580 and ∼520	Murata et al. (1959); Federico et al. (1998); Scholz et al. (2011); De Mello and Bilal (2012); Menezes et al., 2016; Aranha et al. (2018)
Jiajika Pegmatite, China	Microcline, albite, muscovite, quartz	Lepidolite, spodumene, beryl, columbite-group minerals; cassiterite, tourmaline, garnet	∼200	Jiankang et al. (2013); Wang et al. (2021); Zhu et al. (2023); Gao et al. (2024)
Fregeneda–Almendra pegmatitic field in Spain and Portugal	Quartz, K-feldspar, albite, muscovite,	Tourmaline, andalusite, garnet, Fe-Mn phosphates, montebrasite, petalite, spodumene, lepidolite	∼300	Roda et al. (2007); Roda-Robles et al. (2010), 2023

by Jahns and Burnham (1969). This type of pegmatite is concentrically zoned and graded inward from zones rich in feldspar, through intermediate zones containing rare element minerals, toward a core strongly enriched in quartz (Cameron et al., 1949; Jahns, 1955; Kesler et al., 2012). Grain size increases drastically inwards due to more rapid diffusion through the low-viscous, flux-enriched liquid (Bartels et al., 2011). Unzoned pegmatites tend to occur in association with host rocks of high metamorphic grade in the stability field of kyanite and spodumene (Horton et al., 1987). This type of pegmatite is relatively narrow and long (1 m–50 m wide and up to 1 km in length; Lentz, 1992), and the distribution of grain sizes and mineralogy is largely homogeneous (Kesler, 1961; Swanson, 2012; London, 2014).

3. Genesis of granitic pegmatitic melts, and their syn-crystallization modification, and post-crystallization evolution

3.1. Unraveling the genesis of granitic pegmatitic melts

The complexity of pegmatite genesis defies a universally accepted model, as its diverse features resist a singular explanation (Simmons and Webber, 2008). The pegmatite-forming process constitutes a continuous physiochemical transition, commencing from magma, traversing through granitic magma cooling, and extending into hydrothermal conditions (Thomas and Davidson, 2007). Previous studies, employing mineral chemistry, fluid inclusions, and experimental phase equilibria, introduced varied models reliant on bulk compositions, depths, and cooling histories (London and Kontak, 2012).

Since the late 19th century, efforts to elucidate the formation processes of intricate textures and uncommon minerals in massive granite-derived pegmatites have persisted. Brögger (1890) proposed internal reactions between a silicate melt and water vapour in the magmatic chamber as the genesis of most pegmatites. A model proposed by Cameron et al. (1949) attributed pegmatite chemical evolution to fractional crystallization. Later, two concepts emerged to explain granitic pegmatite formation (London, 2008). According to experimental findings, pegmatites form via equilibrium crystallization of coexisting granitic melt and hydrous fluid at or slightly below the hydrous granite liquidus (Jahns and Burnham, 1969; Jahns and Tuttle, 1963). During the 1970s and 1980s, the dominant model for pegmatite formation suggested that they originate in the late stages of granitic magma crystallization, with residual melts consisting of both silicate melt and water vapour in equilibrium (Jahns, 1955, 1982; Jahns and Burnham, 1969).

3.1.1. Fractional crystallization of a granitic magma at the pluton scale

The most widely accepted model of pegmatite formation is by fractional crystallization of a granitic pluton (Cameron et al., 1949; Jahns, 1953; Jahns and Burnham, 1969; Černy1991a; London, 2005, 2008; Yuan et al., 2018). In the fractional crystallization process, the primary minerals that crystallize from the melt are alkali feldspar, sodic plagioclase, quartz, and smaller amounts of muscovite or biotite. As these silicate minerals form, they incorporate elements such as Si, Al, K, Na, O, and minor amounts of Fe and H_2O from the melt. During fractional crystallization, fluid (H_2O), flux (B, F, and P), and incompatible element concentrations surge in the residual magma (Trueman and Černý, 1982; Linnen, 1998; Breaks et al., 2005; London, 2005, 2018; Simmons and Webber, 2008). The late residual fraction of silicic melt, viewed as the medium forming pegmatite, is expelled from crystal-laden mush to create small pools within the source granite or extruded dikes (London, 2005). This model implies even upper mantle-derived mafic magma contribution during the final stage of fractional crystallization.

3.1.2. Direct formation via anatexis of rocks in the presence of fluids

Crustal anatexis, prevalent during high-grade metamorphism in the lower to middle crust, has been linked to direct pegmatite formation during the anatexis of adjacent metasedimentary and metaigneous rocks (Simmons et al., 1995, 1996, 2018; Falster et al., 1997, 2005; London, 2005; Martin and De Vito, 2005; Webber et al., 2019; Lv et al., 2021). Peraluminous pegmatitic melts are supposed to be derived directly from metasediments, not genetically tied to fractional crystallization of magma. Evaporite-rich metasedimentary rocks may introduce fluxing components such as boron and lithium into pegmatitic melts. Thus, low-degree partial melts can directly generate pegmatite melts. Some pegmatites in the Oxford County pegmatite field in western Maine were formed by direct anatexis (Webber et al., 2019, 2023; Simmons et al., 2016, 2024). This anatexis model is supported by trace element analyses of Li, Rb, Sr, Cs, B, and Be, as well as chemical modelling of metasediments and leucosomes from migmatites in western Maine, as detailed by Simmons et al. (2016) and Webber et al. (2023). Additionally, high overburden pressure during orogenesis has been proposed as another potential cause of anatexis (e.g., Mukherjee, 2013).

3.1.3. Liquid immiscibility

Liquid immiscibility in hydrous silicate melts, considered a key process in the formation of pegmatitic parental magmas, arising from the parent magma during its differentiation (Peretyazhko, 2010; Thomas et al., 2012; Zagorsky et al., 1999; Müller et al., 2018). This process is distinct from the magmatic-hydrothermal model, demonstrating that immiscible hydrous silicate melt evolves during differentiation. Immiscibility, demonstrated by experimental and fluid inclusion studies, plays a role in enriching granitic melts with volatile and fluxing components (Thomas et al., 2000; Veksler and Thomas, 2002; Thomas and Davidson, 2013). Initial closed-system crystallization involves crystallization of feldspar and quartz, forming graphic intergrowths. Further cooling induces enrichment in volatiles, leading to melt-melt immiscibility, especially involving H_2O, Li, Be, B_2O_3, CO_2, F, Cl, S, Rb, Cs, W, Nb, Ta, and Sn (Thomas et al., 2000). Gradual transformation results in the formation of hydrosilicate liquids, silicate, and silica gel. Liquid immiscibility, crucial for extreme rare element enrichment, typifies late-stage pegmatite formation (Smirnov, 2015).

3.2. Evolution with syn and post-crystallization modification

Several studies emphasize syn-crystallization modification of pegmatitic melt and post-crystallization evolution happens due to hydrothermal fluid interaction (Černý, 1972; Linnen and Williams-Jones, 1994; Badanina et al., 2015; Dostal et al., 2015; Ballouard et al., 2020a, b; Kaeter et al., 2018; Wu et al., 2018; Ballouard et al., 2020a). This modification, is pivotal for the genesis of economically significant minerals in pegmatites (Černý, 1972), involves hydrothermal fluid interaction at late pegmatite genesis stages, potentially yielding metasomatic transformation. Hydrothermal fluids play a vital role in the formation of pegmatite-related rare metal deposits by mobilizing elements around granitic intrusions through processes like exsolution and metasomatism (Thomas et al., 2011a,b; Badanina et al., 2015; Dostal et al., 2015; Ballouard et al., 2020a; Kaeter et al., 2018; Wu et al., 2018). Often, magma and hydrothermal fluids are immiscible (Ballouard et al., 2020a, b). Components like H_2O, B, F and P play a significant role in lowering pegmatite formation temperature, enhancing miscibility among less soluble constituents (London, 1986; London et al., 1988, 1997; Keppler, 1993; Thomas et al., 2000; Sowerby and Keppler, 2002). Melt-fluid immiscibility during the magmatic-hydrothermal transition proves to be an effective mechanism for rare metal mineralization in pegmatites (Zhou et al., 2023). Table 3 summarizes some selected studies on syn and post-crystallization modifications in global Pegmatites.

In contrary, London (1992, 2005) argued against the necessity of a hydrous vapour phase for pegmatitic texture development. Others (e.g., Masoudi and Yardley, 2005; Van Daele et al., 2018 from the Borujerd complex of western Iran and Rwamagana-Musha-Ntunga pegmatite--quartz vein field of East Rwanda, respectively) suggested the potential mixing of magmatic and metamorphic fluids during pegmatite development. Additional reports indicate the mixing of meteoric fluid with

Table 3
Some selected Studies on Syn and Post-Crystallization Modifications in Pegmatites.

Author/s and year	Locality or pegmatite field	Key interpretation related to modifications in Pegmatites
Chadwick (1958)	New England, USA	The various pegmatites developed by several mechanisms. Furthermore, individual pegmatites commonly exhibit evidence for more than one process.
Černý (1972)	Tanco pegmatite	Late hydrothermal activity produced a series of secondary minerals in the spodumene-rich zones of the Tanco pegmatite
Kinnaird (1985)	Jurassic alkaline anorogenic granitic ring complexes in central Nigeria	The contribution of post-crystallization acid metasomatic fluid to the mineralization of ore minerals such as monazite, zircon, and ilmenite, followed by cassiterite, wolframite, columbite, siderite, and rutile.
Shearer et al. (1986)	Black Hills, South Dakota. USA	Migration of pegmatite-derived fluids out of pegmatite bodies and into the surrounding country rock can form extensive alteration aureoles.
Morgan and London (1987)	Tanco pegmatite, Bernic Lake, Manitoba	The occurrences of metasomatic alteration of pegmatite under the presence of fluids
Linnen and Williams-Jones (1994)	Nong Sua, Thailand	The two dominant stages of Sn-W-Ta-Nb mineralization are: (1) the early stage, which forms directly from the magmatic melt, and (2) the later stage, which involves the formation of W-rich minerals through Fe-Mn-rich fluids.
Uher et al. (1998)	Prasivá granitic pegmatites, Slovakia	The hydrothermal overprint of the Prasivá pegmatites was caused by external, low-temperature CO_2-rich aqueous solutions of magmatic-metamorphic origin
Thomas et al. (2003)	Ehrenfriedersdorf Complex, Germany	Detailed analyses of melt and fluid inclusions combined with an electron-microprobe survey of boron-bearing minerals reveal the evolution of boron in a highly evolved peraluminous granite-pegmatite complex and the associated high- and medium-temperature ore-forming hydrothermal fluids.
Palinkaš et al. (2014)	Mina do Santino and the Jacú pegmatites in the Borborema Pegmatite Province in northeastern Brazil	After minerals such as feldspars and beryl were deposited under magmatic conditions, they interacted with hydrothermal fluids, becoming unstable. This interaction led to the formation of a new hydrothermal mineral paragenesis, which included euclase, bertrandite, kaolinite, and quartz, that overprinted the earlier magmatic minerals
Rao et al. (2017)	The Nanping No. 31 pegmatite (Fujian Province, southeastern China)	The study suggests that the re-enrichment of Li during the post-magmatic stage likely increased the solubility of Ta in the hydrothermal fluids of the granitic pegmatite. This implies that the hydrothermal alteration processes not only affect the distribution of Li but also influence the behavior of other rare elements like Ta in the pegmatite system.
Kaeter et al. (2018)	Southeast Ireland	The study reveals that hydrothermal fluids significantly impact the mineralogical evolution during the magmatic-hydrothermal transition. Ta and Nb are fractionated differently during the hydrothermal process. Ta is preferentially concentrated and redeposited by halogen-rich aqueous fluids, leading to Ta-enriched mineralization. This fractionation is observed in both the magmatic and hydrothermal stages, with hydrothermal fluids playing a crucial role in the remobilization and redeposition of Ta.
Wu et al. (2018)	Shangdan domain of the North Qinling Orogenic Belt, China	Hydrothermal alteration of primary uraninite involved multiple stages of fluid-assisted metasomatism.
Yin et al. (2020)	The Bailongshan pegmatite district in south Xinjiang Province, NW China,	Hydrothermal fluids caused the development of Cs- or Na-enriched veinlets in beryl and Mn- and Ta-enriched veinlets in columbite-group minerals. These alterations reflect the complex chemical interactions between the pegmatitic magma and the hydrothermal fluids, which were rich in Li, F, Cs, and Ta.
Ballouard et al. (2020a)	Orange River pegmatite belt, Namaqualand, South Africa	The study emphasizes the complex interplay between magmatic and hydrothermal processes in the formation of pegmatite-related rare metal deposits. It indicates the alteration of primary minerals in the pegmatites through hydrothermal fluids in several stages.
Bhandari et al. (2023)	Yamrang Pegmatite, Eastern Nepal	Alkali-enriched fluids exsolved from the pegmatite, leading to the formation of miarolitic cavities and the crystallization of aquamarine. This process resulted in the development of hydrothermal beryl, characterized by its sodic to Li-Cs composition, tabular to acicular habit, and weak compositional zoning. The

(continued on next page)

Table 3 (*continued*)

Author/s and year	Locality or pegmatite field	Key interpretation related to modifications in Pegmatites
		hydrothermal stage significantly influenced the pegmatite's mineralogy and texture.
Xu et al. (2024)	Songpan–Ganzê orogenic belt, Eastern Tibet	The hydrothermal alteration, particularly metasomatism, leads to the release of elements like Ta, Nb, Sn, and W from primary minerals (spodumene, alkali feldspar, and columbite-group minerals) into the reactive media (melt/fluid). This redistribution results in the depletion of these elements in early-formed minerals but sets the stage for their subsequent mineralization.

magma at low pressure for pegmatite production (Thomas et al., 2003; Kaeter et al., 2018).

4. Geochemical signature of granitic pegmatitic melt

The chemical composition of granitic pegmatitic melt includes fluids, volatile fluxing components, iron, and molecules, including rare elements.

4.1. Role of fluids, volatiles, and fluxing components

The majority of granitic pegmatites represent "simple" chemical compositions that represent the system $NaAlSi_3O_8$–$KAlSi_3O_8$–Al_2O_3–SiO_2 (London and Morgan, 2012). The profound role of water in pegmatite formation, as emphasized by Niggli (1920), finds support in the evidence provided by Jahns and Tuttle (1963) and Jahns and Burnham (1969), suggesting pegmatite formation occurs through equilibrium crystallization of coexisting granitic melt and hydrous fluid. Using the phase relations in the peralkaline [$Al_2O_3 < (Na_2O + K_2O)$] portion of the Na_2O–Al_2O_3–SiO_2–H_2O system, Mustart (1972) further elucidated the potential of peralkaline melts to dissolve elevated concentrations of H_2O as temperature decreases. However, experimental, fluid inclusion, and melt inclusion studies emphasize the pivotal influence of water in pegmatitic melt, impacting mineral melting and crystallization dynamics (e.g. Fig. 2). Water, along with other volatiles (H_2O, F and Cl) and semi-volatiles (B_2O_3 and P_2O_5), not only reduces the viscosity of aluminosilicate melts but also enhances ion transfer through the melt to promote unusually large crystal growth (see Thomas et al., 2006; for details). The ability of water to transport incompatible elements contributes to the crystallization of residual melt until the separation of water vapour and silicate-rich melt (Fig. 2). The interaction between water and silicate-rich melt during this phase yields distinctive igneous textures (Simmons and Webber, 2008). Additionally, volatile components like carbonate/bicarbonate/CO_2 play a significant role in granitic pegmatite evolution (Thomas et al., 2011a,b; Liu et al., 2022a, 2022b), facilitating low-viscosity melts and fostering large crystal growth (Thomas et al., 2011a,b).

Granitic magma, recognized as a complex suspension, composes dissolved gases, including ~6% water in residual magma (Roedder, 1992), along with Cl, F, and S gases and acids (Tyrrell, 1978). Some magmatic-hydrothermal fluids display a dominance of coexisting vapour and complex multiphase brines (Kamenetsky et al., 2002; Webster et al., 2004). Continuous cooling of volatile-enriched pegmatitic melt leads to the development of two or more melt fractions due to

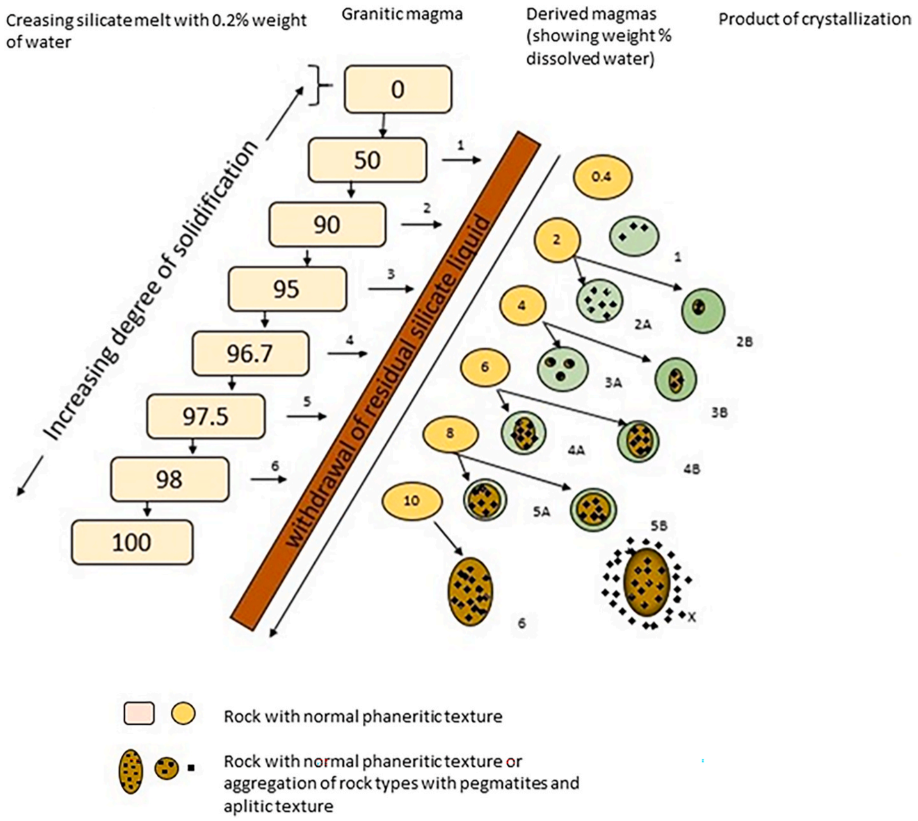

Fig. 2. A schematic diagram showing the crystallization of granitic magma and withdrawn residual silicate liquid at increasing degrees of consolidation of a melt initially containing 0.2 wt % H_2O (Modified after Jahns and Burnham, 1969).

their propertis of liquid immiscibility, characterized by lower viscosity, facilitating separation from the larger magma body (Thomas et al., 2000). Below 750 °C, granitic melt typically contains substantial fluxing components, especially F and alkali metals (Smirnov, 2015). Experimental studies by Kovalenko (1979) showed that under H_2O-saturated conditions, the granite minimum temperature drops to 550–600 °C with the addition of fluorine. Dingwell et al. (1996) suggested a decrease in the temperature of the quartz-albite-orthoclase (haplogranite) system equilibrium with an aqueous fluid containing 7–9 wt.% B_2O_3 to 620–640 °C. Several authors (e.g. Taylor et al., 1979; Linnen and Williams-Jones, 1994; Webster et al., 1997; Zaw, 1998; Thomas et al., 2000, 2012; Fei et al., 2018; Wang et al., 2023; Lv et al., 2024) highlighted the incorporation of a number of potential flux components, which may include H_2O, $OH-$, CO_2, HCO^{-3}, CO_2^{-3}, SO_2^{-4}, PO_3^{-4}, H_3BO_3, F, and Cl, as inclusions in different mineral phases in pegmatites. Fluid inclusion analysis by Smirnov (2015) revealed that pegmatite minerals often contain trapped melts with high alumina contents, with F playing a crucial role in the glasses of melt inclusions, reaching up to 5 wt%.

4.2. Rare elements concentrations

During the continuous fractional crystallization of magma, the residual melt eventually becomes saturated in incompatible elements and fluxing components (Thomas et al., 2000; Thomas et al., 2019; Troch et al., 2022). The high enrichment in granitic pegmatites makes them a classic source for a diverse range of trace elements such as Li, Rb, Cs, Be, Ga, Sc, Y, REE, Sn, Nb, Ta, U, Th, Zr, and Hf. Fractional crystallization may enrich trace elements in pegmatites up to some wt.% levels (e.g. London, 2008; Fredriksson, 2017). Most pegmatites, though compositionally similar to simple granites, lack evidence for fluxing components such as B, P and F, as well as high concentrations of normally rare elements like large-ion lithophile elements (LILE) and high field-strength elements (HSFE) (London, 1992). For instance, a positive correlation exists between Li, Rb, Cs, F, Be, Ga, B, P, Mn, Nb, Ta, Zr, Hf, Sn, and U with increasing differentiation of peraluminous pegmatites (e.g., Černý and Ercit, 1985). Shaw et al. (2016) argued that rare-metal pegmatites are also distinguished by their bulk-rock and mineral chemistry, including a more peraluminous character and enrichments in Rb, Li, Cs, Be, Nb and Ta. London and Kontak (2012) suggested that the process of rare-element enrichment in pegmatites appears to occur in a closed system, originating from a small fraction of residual silicate liquid derived from a much larger magma body. In contrast, hydrothermal fluids in chemically open systems can contribute to the addition of rare elements (London and Morgan, 2012).

5. Cooling history, rates of crystal growth and P-T evolution of granitic pegmatites

5.1. Influence of cooling rate on the formation of pegmatitic textures

The dynamics of cooling in shallow-level pegmatites, as proposed by various researchers, span from weeks to years based on their respective sizes (e.g., Chakoumakos and Lumpkin, 1990; Webber et al., 1997, 1999; Morgan and London, 1999; London et al., 2012a). It is widely acknowledged that the principles governing mineral crystallization in conventional magmatic systems can not be directly applied to pegmatites. For instance, experimental studies on quartz and feldspar crystallization in granitic melts (e.g., Swanson and Fenn, 1986, 1992; MacLellan and Trembath, 1991; Fenn, 1977, 1986) have revealed that skeletal and graphic morphologies denote rapid crystal growth from a highly undercooled melt (Simmons and Webber, 2008). Textural relationships in pegmatites, such as needle-like, skeletal, branching, and wedge-shaped crystals, indicate rapid cooling, higher growth rates, and larger degrees of undercooling, with fewer nucleation sites. In contrast, tabular to equant crystal forms are indicative of slower cooling rates, lower growth rates, smaller degrees of undercooling, and abundant nucleation sites. Notable examples include the Harding pegmatite in New Mexico (Chakoumakos and Lumpkin, 1990) and the George Ashley, Mission, Stewart, and Himalaya dikes in San Diego County, California (Webber et al., 1997, 1999), which underwent rapid cooling, reflecting unusual growth rates in the cooling history of the pegmatites (Simmons and Webber, 2008). Černý et al. (2005) suggested that even the Tanco pegmatite, with a thickness of 100 m appears to have cooled rapidly within decades to a maximum of a few hundred years. Webber and Simmons (2007) utilized a cooling model along with the parameters provided by Černý et al. (2005), which include a thickness of 100 m, an emplacement temperature of 700 °C, an emplacement depth of 10 km, and country rock temperatures ranging from 25 °C to 300 °C. They calculated that the Tanco pegmatite cooled from 700 °C to approximately 450 °C over a period of about 700 to 1000 years.

Rapid cooling rates in pegmatites challenge the prevalent notion that large crystals in pegmatites result from very slow rates of cooling and crystal growth. The phenomenon of rapid cooling with the formation of large crystals (e.g., McBirney and Russell, 1987; London, 1992, 1999, 2005) is explained by the concentration of incompatible elements, fluxes, volatiles and rare earth elements in the residual magma during the initial stages (e.g., Dingwell et al., 1996; Linnen et al., 2012). The presence of fluxes and volatiles, lowering crystallization temperature, reducing nucleation rates, melt polymerization and viscosity, and increasing diffusion rates and solubility, is considered crucial for the development of large crystals and pegmatitic textures (Simmons and Webber, 2008). Consequently, granitic pegmatite grains exhibit extreme variation in size (Jahns, 1955; Sinclair, 1995). Given that a majority of pegmatites form at shallow depths of the crust (around 3–5 km, Kozłowski, 1978), the H_2O solubility in aluminosilicate melts strongly depends on pressure over temperature (e.g., Holtz et al., 2001). Holtz et al. (2001) noted that at the eutectic point (2 kbar/680 °C) in the quartz-albite-orthoclase-water system, the H_2O content is about 6.4 wt% and the viscosity is approximately 105.5 Pa s. Under such high-viscosity conditions, the formation of typically coarse-grained or giant-textured pegmatites becomes challenging (Simmons and Webber, 2008). Pegmatite evolution involves disequilibrium crystallization from an undercooled, flux-bearing granitic melt, which is necessarily flux-rich and does not require the presence of an aqueous vapour phase (Morgan and London, 1999; London, 2005; Simmons and Webber, 2008).

London (2005, 2018) proposed a model to address the viscosity problem, assuming a boundary layer enriched in incompatible fluxing components along the margins of the growing crystal front. Fluxing components aid in lowering the viscosity and solidus of granitic melts, enhancing the solubility of components that would otherwise precipitate as accessory minerals, and promoting the rapid growth of large, perfect silicate crystals (London et al., 2012a). The enrichment of fluxing components in the pegmatitic melt not only facilitates rapid diffusion of elements into the crystal structure of the growth surfaces (London, 2009; London, 2014) but also influences the formation of fluid inclusions in the larger host crystals (London, 2015). When crystal formation begins, incompatible components, including the fluxes, are rejected at the growing crystal interface of quartz and feldspar (London, 2005). These components then concentrate along the margins of the growing crystal front, forming a fluxed boundary layer of melt. Although the overall concentration of fluxes in the pegmatitic melt is low, a boundary layer can form if the diffusion of excluded components through the melt is slower than the rate of crystal growth. This boundary layer, being richer in fluxes, may exhibit a lower solidus temperature and increased silicate-H_2O miscibility. A model based on the high viscosity of the pegmatite-forming medium (supercooled silicate liquid, gel, or glass) was proposed by London (2005) to explain why granitic pegmatites are more common than those of basic or alkaline composition. The author suggested that due to the higher viscosity of granitic liquids, the diffusion of elements necessary to nucleate crystals decreases. The higher viscosity of granitic liquids also impedes the diffusion of excluded components back into the melt, promoting boundary layer formation that results in pegmatite textures. Alternatively, considering metasomatic processes, Beus (1983) proposed a model for the giant growth of crystals embedded in hard rock.

After conducting experimental studies at 480–700 °C and 220–960 MPa using H_2O-saturated melts of a typical granitic composition as well as granitic melts enriched in lithium (8800 ppm), Maneta and Anderson (2018) showed that euhedral quartz and alkali feldspar megacrysts crystallized over a period of hours with an average growth rates ranging from 3 (Li-free charges) to 41 cm/year (Li-enriched charges) for quartz and from 18 (Li-free samples) to 58 cm/year (Li-enriched samples) for alkali feldspars. Using the above experimental data, these authors argued that crystals formed from a silicate melt in the presence of a coexisting aqueous phase crystallize rapidly. In addition, crystals formed in miarolitic pockets can also crystallize rapidly.

5.2. *Pressure-temperature (P-T) evolution*

Determining the *P-T* evolution of many granitic pegmatites is challenging due to the absence of proper mineral assemblages for thermobarometry. Nevertheless, several studies attempted to speculate on the *P-T* evolution of pegmatites using experimental data, stable isotopic data, fluid inclusion analysis, and thermal modelling (e.g., Jahns and Burnham, 1969; Babu, 1969; Taylor et al., 1979; Kosukhin et al., 1984; Simmons et al., 1987; Bakumenko and Konovalenko, 1988; Chakoumakos and Lumpkin, 1990; Sirbescu and Nabelek, 2003a, b; London et al., 2012a; Fei et al., 2021; Wang et al., 2023). Table 4 summarizes the estimated P-T condition of selected pegmatites/pegmatite fields in the world throughout the history of pegmatite studies.

Jahns and Burnham (1969) proposed that pegmatites crystallize at or near the hydrous minimum melt temperatures of about 600 °C. Babu (1969), based on the chemical compositions of associated granitic gneisses, argued that crystallization of different mineral varieties in the pegmatite in the Nellore Mica Belt, Andhra Pradesh, India, occurred between 760 and 300 °C. The colour-temperature relationships and the associated minerals in the pegmatite prompted Babu (1969) to propose that the crystallization temperature range for tourmaline is between 760 °C and 450 °C, while for beryl, it is between 500 °C and 400 °C. Muscovite indicates a minimum crystallization temperature of 500 °C and 435 °C, based on the relationship within the paragonite-muscovite solid solution (Babu, 1969). Stable isotopic studies on pegmatites from San Diego County, California, led Taylor et al. (1979) to argue that temperatures of pegmatite melt emplacement ranged between 730 °C and 700 °C. The authors suggested that supersolidus crystallization

Table 4
Estimated *P-T* condition of selected pegmatites/pegmatite fields in the world.

Reference	Pegmatite/pegmatite field	*Used methods*	*Crystallization conditions*	
			P	T
Brotzen (1959)	Stockholm, Sweden	Considering mineral solid solutions' stability	–	600 °C
Jahns and Burnham (1969)		Experimental studies	-	Hydrous minimum melt temperatures of about 600 °C
Babu (1969)	Nellore Mica Belt, Andhra Pradesh, India	Mainly based on mineral compositions	–	760–300 °C Crystallization of: - Tourmaline 760 to 450 °C - Beryl is 500 °C–400 °C - Muscovite 500 to 435 °C
Taylor et al. (1979)	San Diego Co., California	Considering oxygen isotope fractionations between minerals	–	730 to 700 °C - Aplite zone in this pegmatite occurring around 565 °C - Gem pocket formation in the relatively narrow temperature range of about 40 °C (approximately 565–525 °C)
Kosukhin et al. (1984)	Russia	Fluid and melt inclusion analysis	3.0–0.5 kbar	Granite pegmatites which contain mineralized cavities (miaroles) crystallize at 750 - 515 °C
Simmons et al. (1987)	South Platte, Colorado	Two-feldspar thermometry		550–500 °C
Bakumenko and Konovalenko (1988)	SW Pamirs	Fluid and melt inclusion analysis		Crystallization of miarolitic quartz 510–505 °C
Chakoumakos and Lumpkin (1990)	Harding pegmatite. Taos county, New Mexico, USA	I) the experimentally determined liquidus, solidus and phase assemblages for a bulk sample of the pegmatite, 2) isochores for CO_2-H_2O-NaCI fluid inclusions in quartz and beryl	3.3–3.5 kbar	650 °C
Morgan and London (1999)		Two-feldspar thermometry.		
Frindt and Poutiainen (2002)	Gross Spitzkoppe Granite Stock, Namibia	Fluid inclusion analysis	0.9 kbar	Crystallization and fluid entrapment during cooling from high temperatures (around 550 °C) down to lower temperatures around 170 °C
Kontak et al. (2002)	Peggys Cove, Nova Scotia, Canada	Fluid inclusion analysis	3–3.5 kbar	600–650 °C
Sirbescu and Nabelek (2003a, b)	Black Hills, South Dakota	Fluid inclusion analysis	2.7 kbar	~400–350 °C
Li et al. (2013)	Jiashan–Xiangshui Fault, china	Ti in zircon thermometry		730–840 °C
Fei et al. (2021)	Songpan-Garze Fold Belt, southwestern Sichuan province, China	Fluid inclusion analysis	>4.7 kbar	741 to 658 °C
Knoll et al. (2023)	Austroalpine Unit Pegmatite Province (Eastern European Alps)	Studying of metamorphic history of surrounding metamorphic rocks	3–4 kbar	500–570 °C
Wang et al. (2023)	Lhozhag, eastern Himalaya	Studying of metamorphic history of surrounding metamorphic rocks	3.1	720–650 °C

began with the basal aplite zone in that pegmatite occurring around 565 °C, whereas the subsolidus formation of gem-bearing pockets took place at approximately 565–525 °C in a nearly closed system.

Kosukhin et al. (1984) demonstrated that the minerals of granite pegmatites, containing mineralized cavities (miaroles), crystallize between 515 and 750 °C and 0.5–3.0 kbar. Bakumenko and Konovalenko (1988) reported the lowest temperatures of homogenization of melt inclusions (505–510 °C) from miarolitic quartz from the Vezdarinskaya vein (SW Pamirs). Chakoumakos and Lumpkin, (1990) found that the crystallization of the Harding pegmatite in Taos County, New Mexico, USA, occurred at 650 °C and 3.3–3.5 kbar and subsequently cooled isobarically to 550 °C. This conclusion was based on experimentally determined liquidus and solidus temperatures, phase assemblages for a bulk sample of the pegmatite, and isochores for CO_2-H_2O-NaCl fluid inclusions in quartz and beryl.

Simmons and Webber (2008) summarized the crystallization temperature conditions of various granitic pegmatites. They noted that the intermediate zones of pegmatites in South Platte, Colorado, recorded temperatures between 550 °C and 500 °C (Simmons et al., 1987) based on two-feldspar thermometry. In contrast, the Little Three pegmatite in California showed temperatures of approximately 400 °C–435 °C near the margins, 350 °C–390 °C close to the pegmatite pocket zone, and a sharp decline to 240 °C–275 °C within the pockets (Morgan and London, 1999) Nabelek et al. (1992a, b) estimated that the equilibration temperatures for coexisting quartz and K-feldspar in the cores of various pegmatites in the Black Hills, South Dakota, were about 350 °C. For the Li-bearing Tin Mountain pegmatite in the same region, Sirbescu and Nabelek (2003a, b) proposed that crystallization occurred from fluid-rich, compositionally complex melts at around 400 °C–350 °C. The lower crystallization temperatures were attributed to the combined fluxing effects of Li, B, P, H_2O, and carbonate anions (Sirbescu and Nabelek, 2003a, b). Evidence from thermal models combined with mineral compositions, as reported by London et al. (2012a), indicates that crystallization in pegmatites starts at approximately 450 °C, which is about 200–250 °C lower than the liquidus temperature where crystallization is expected to begin. The Lijiagou spodumene pegmatites in the Songpan-Garze Fold Belt, southwestern Sichuan Province, China crystalized at a high-temperature of 660–740 °C at moderate pressure of 4.7–6 kbar (Fei et al., 2021). Wang et al. (2023) attempted to study the *P-T* condition of pegmatite after considering the *P-T* evolution of host metamorphic rocks and the mineralogical evolution of pegmatites in Lhozhag, eastern Himalaya. The authors interpreted the crystallization temperature of the pegmatite to be around 580 °C at a pressure of 4 kbar.

6. Classification scheme for granitic pegmatites

In 1920, the Swiss mineralogist Niggli proposed a classification system for pegmatites that consisted of two levels: types and sub-types, which were categorized according to their chemical composition and mineral content. He highlighted that the distinct mineralogy and texture of pegmatites are mainly influenced by the type and amount of volatile components found in the pegmatite melts. Throughout the last century, efforts were made by Russian and French authors to classify pegmatites. Later, in 1930, Russian mineralogist and petrologist Fersman introduced the first internationally recognized classification of pegmatites. This classification was based on the thermal evolution of pegmatite melts.

Notably, Landes (1933) categorized pegmatites into acid, intermediate, and basic varieties. Subsequent classifications considered emplacement depth, metamorphic relationships, granitic activity, geochemistry, and the association with pegmatite-host rocks (e.g. Ginsburg and Rodionov, 1960; Ginsburg et al., 1979; Černý, 1991a, b; Zagorsky et al., 1999; Fuchsloch et al., 2018). Additionally, internal characteristics such as zoning, feldspar composition, grain size variation, and textural patterns were also included as classification criteria (Abdelfadil et al., 2016). The classification of granitic pegmatites is acknowledged to be more intricate than that of other igneous rocks. The following section provides a summary of each proposed classification scheme. A summary of existing classification schemes of granitic pegmatite is available in Table 5.

6.1. *Classification based on depth of emplacement*

Pegmatites were classified into four geological classes, considering factors such as depth of emplacement, metamorphic relationships, and their associations with granitic plutons (Ginsburg and Rodionov 1960; Ginsburg et al., 1979).

These classifications include (i) very deep-seated uranium–REE pegmatites (emplacement deeper than 10–11 km), (ii) great depth for mica-bearing pegmatites (emplacement at 7–11 km), (iii) moderate depth for rare-metal pegmatites (emplacement at 3.5–7.0 km), and (iv) minor depths for rock-crystal pegmatites (emplacement depth at 1.5–3.5 km) (Beskin and Marin, 2018).

6.2. *Classification based on P-T conditions*

Fersman (1930) attempted to classify granitic pegmatites based on crystallization temperature, considering the thermal stability of minerals and mineral assemblages. The above author referred to the crystallization temperature starting with ~700 °C as 'ordinary allanite-monazite pegmatites' and the lower limit representing ~200 °C as 'zeolite pegmatites'. Crucial temperature boundaries at ~600 °C and ~400 °C, known as the β-/α-quartz transition (Fig. 4) and the critical point of water, respectively, were used to divide the thermal evolution into pegmatitic (600 °C), pneumatolytic (600–400 °C), and hydrothermal (400 °C) stages (Fig. 4). Fersman (1930) outlined ten main thermal types of pegmatites and added an eleventh type for "fillings in miarolitic cavities." He also described three compositional lineages: pure (no wall rock interaction), contaminated (affected by wall rocks), and migmatitic (intense interaction with wall rocks). These classifications are further divided based on mineralogy. He outlined ten main thermal types of pegmatites, with the pure (non-contaminated) lineage subdivided into 18 sub-types based on mineralogy and the contaminated lineage divided into 9 sub-types (Fig. 4). He added an eleventh type for "fillings in miarolitic cavities." He described three compositional lineages: pure (no wall rock interaction), contaminated (affected by wall rocks), and migmatitic (intense interaction with wall rocks). Fersman (1930) used temperature-indicative minerals and mineral parageneses to establish the temperature of pegmatites, noting that 250 indicative minerals could be organized into a "mineralogical-thermal evolution scheme" for this purpose. Despite the value of temperature-based classification, he acknowledged that factors like melt origin and contamination also play a significant role. Therefore, he superimposed compositional lineages on the temperature classification for a more comprehensive framework, recognizing that most pegmatites crystallize across multiple thermal intervals.

Černý (1991a) revised the above classification, considering emplacement depth, metamorphic grade, and minor element content, resulting in four main categories: Abyssal, Muscovite, Rare Earth element, and Miarolitic pegmatites (Table 6). Abyssal is associated with high grade, intermediate to high pressure facies, analogous to an upper amphibole facies environment (~700–800 °C and 4–9 Kbar), while muscovite is linked to high-pressure and low-temperature facies similar to amphibolite-barrovian kyanite facies (580–650 °C and 5–8 kbar; Fig. 3). Rare elements are associated with low temperature and low pressure, resembling amphibolite - upper greenschist facies (500–600 °C and 2–4 kbar), and the miarolitic class indicates shallow levels (1–2 kbar; Fig. 3).

6.3. *Classification based on composition*

Niggli (1920) proposed a two-level classification based on chemical characteristics and mineralogy. In this classification, the specific

Table 5

Summary of existing classifications schemes of granitic pegmatites (modified after Müller et al., 2022)

Author/s	1st order classification criterion	2nd order classification criterion	3rdorder classification criterion	Evolution
Niggli (1920)	Geochemistry	Mineralogy	–	Not well constrained
Fersman (1930)	Temperature	Geochemistry	Mineralogy	Temperature along not sufficient
Landes (1933)	Geochemistry	Structure	Mineralogy	Too simple, not well-constrained
Bjørlykke (1937)	Geochemistry, genesis	Mineralogy	Mineralogy	Limited to rare metal pegmatites of the NYF family
Vlasov (1952, 1961)	Structure, mineralogy	Mineralogy		Too simple, not well-constrained
Ginsburg and Rodionov (1960); Ginsburg et al. (1979); Ginsburg (1984)	Emplacement depth	Structure (presence or absence of miarolitic cavities)	Geochemistry	It presupposes that the metamorphic grade of the wall rock corresponds to the P-T conditions at the time of pegmatite emplacement
Schneiderhöhn (1961)	Genisis (anatectic vc. Magmatic)	Geochemistry	Geochemistry	Too simple
Černý (1991a) and Černý and Erict (2005)	Mixture of emplacement depth structure and mineralogy	Geochemistry	Mineralogy	A mixture of different types of classification criteria in the 1st order
Wise (1999)	Mineralogy	Mineralogy	Mineralogy	Classification of NYF-type pegmatites only
Pezzotta (2001)	Mixture of emplacement depth structure and mineralogy	Mineralogy, geochemistry	Mineralogy	Limited to pegmatites occurring in Madagascar
Zagorsky et al. (1999, 2003)	Emplacement depth	Mineralogy (structure)	Mineralogy (structure)	Emplacement depth is commonly uncertain
Dill (2016)	Mixture of emplacement style, deformation, host rock type, chemical and mineralogical features	Structure	Chemistry	The distinction of different pegmatite types (1storder) is difficult to draw in several classes
Wise et al. (2022)	Mineralogy	Geochemistry	Genesis (magmatic vs. anatectic)	Fall short in accommodating all variations observed in nature, particularly in hybrid or mixed-origin pegmatites

mineralogy and texture of pegmatites primarily determine the type and amount of volatile components. Niggli introduced fifteen pegmatite types associated with granitic and syenitic magmas. In Černý's (1991a) classification, rare-element pegmatites were further categorized into two families (Table 6): the LCT family (Li, Ce, and Ta enrichment) and the NYF family (Nb, Y, and F enrichment). These families were then subdivided based on mineralogical or geochemical characteristics. For instance, the LCT family was divided into four subtypes: beryl, complex (rare-element), albite-spodumene, and albite types, with the beryl type further subdivided into two sub-types: beryl-columbite and beryl-columbite-phosphate (Table 6). Zargorsky et al. (1999) suggested that miarolitic facies can occur to varying degrees in almost any pegmatite sequence. Based on the type of granite plutons, the classification has three main classes based on the aluminum saturation of the parent granite and mineralogy. Based on mineralogy, Wise (1999) classified NYF pegmatites into three classes named peralkaline, metaluminous, and peraluminous. This classification includes six types and nine sub-types. Pezzotta (2001) attempted to classify pegmatites according to old depth-related classification schemes but modified the older classification after considering pegmatite mineralogy, which relates to the pegmatite bulk chemistry. Pezzotta (2001) classified pegmatites into three classes based on emplacement depth structure and mineralogy. According to this classification: *Class I*: Abyssal (K-feldspar and corundum subtypes) is formed at low pressure and high temperature, poorly mineralized but rich in ceramic minerals such as quartz and feldspars. *Class II*: The rare-element class (Beryl, rare earth type, and complex subtypes are included) is the most mineralized and most mineralogically diverse. This class includes NYF and LCT types. *Class III*: NYF miarolitic is formed under a low-pressure regime. This type of pegmatites can be seen at shallow levels, and miarolitic cavities are common. Ercit (2004) found a low degree of correlation between accessory mineralogy and depth of emplacement for NYF pegmatites. Ercit (2004) divided NYF pegmatites into four categories: Abyssal, Muscovite–rare element class, and Miarolite classes. The abyssal class was further divided into two subclasses as the allanite monazite-uraninite subtype and the (Y, REE)-Nb-oxide subtype. Meanwhile, the rare-element class also has three subclasses, namely allanite-monazite, euxenite, and gadolinite.

Černý and Ercit (2005) proposed a classification for pegmatites by combining the systems proposed by Černý (1991a) and Ercit (2004), with several changes that address NYF pegmatite classification and a petrogenetic classification of pegmatites derived from plutons. In Černý and Ercit's (2005) classification, three families were distinguished: (i) the NYF family with progressive accumulation of Nb, Yand F, fractionated from sub-aluminous to meta-aluminous A- and I-granites, (ii) the LCT family, commonly accumulated Li, Cs, and Ta and derived mainly from S-granites and rarely form I-type granite, (iii) mixed by the NYF + LCT family of diverse origin.

Recently, Wise et al. (2022) proposed a classification scheme for pegmatites based on their association with primary accessory rock-forming and rare-element minerals (Table 7), and pegmatites are divided into three main groups as Groups 1, 2 and 3. According to the Wise et al. (2022) classification, the pegmatites of Group 1 are typically enriched in Li, Rb, Cs, Be, Ga, Sn, Ta, Nb, B, P and F. Three types of pegmatites in this group are frequently recognized as (i) beryl phosphate-bearing types, (ii) Li-rich spodumene- or petalite-dominant types, and (iii) bodies with lepidolite or elbaite as the principal Li phase. In the pegmatite Group 2, the most common granitic pegmatites are composed mainly of quartz and feldspar. The presence of small but significant amounts of accessory minerals, such as helvite, magnetite, fluorite or hyalite opal, serves to distinguish them from Group 1 pegmatites. The pegmatite Group 3 is strongly peraluminous, with essential K-feldspar, quartz, and plagioclase, and accessory biotite, muscovite, garnet or tourmaline. The authors suggested that pegmatites belonging to Groups 1 and 2 are generated from the residual melts of S-, A-, and I-type granite magmatism and are also direct products of anatexis. The Group 3 pegmatites are only derived by anatexis.

In evaluating the classification of pegmatites, it is essential to recognize the complexities and evolving nature of the classification systems proposed over the last century. The early works (e.g., Niggli, 1920; Fersman in 1930; Landes, 1933) laid the groundwork by focusing on chemical composition, mineralogy, and thermal evolution. Although pioneering, these schemes were limited by the scientific knowledge of their time. As subsequent researchers built on these foundations, classifications became increasingly sophisticated, incorporating not only chemical and mineralogical data but also emplacement depth, geochemical signatures, and tectonic settings (e.g., Černý, 1991a; Wise, 1999; Ercit, 2004).

However, this increasing complexity also presents challenges. For instance, the classification systems by Černý and Ercit (2005) and Wise et al. (2022) aim to address the diverse origins and geochemical signatures of pegmatites, but still fall short in accommodating all variations

Table 6
Classification of granitic pegmaitte (the table is a modified version after Černý, 1991a; Simmons and Webber, 2008).

Class	Family	Pegmatite types	Pegmatite sub types	Geochemical signature	Metamorphic environment	Relation to granite	Structural features	Example
Abyssal				U, Th, Zr, Nb, Ti, Y, REE, Mo poor (to moderate) mineralization	(upper amphibolite to) low- to high-P granulite facies ~4–9 kb ~700–800 °C	none (segregations of anatectic leucosome)	conformable to mobilized cross-cutting veins	Rae and Hearne Provinces, Sask. (Tremblay, 1978); Aldan and Anabar Shields, Siberia (Bushev and Koplus, 1980)
Muscovite				Li, Be, Y, REE, Ti, U, Th, Nb > Ta poor (to moderate) mineralization, micas and ceramic minerals	high-P, Barrovian amphibolite facies (kyanite-sillimanite) ~5–8 kb ~650-580 °C	None (anatectic bodies) to marginal and exterior	quasi-conformable to cross-cutting	White Sea region, USSR (Gorlov, 1975); Appalachian Province (Jahns et al., 1952); Rajahstan, India Shmakin (1976)
Rare – Element	LCT Poor to abundant mineralization, gem stock industrial minerals	Beryl	Beryl – columbite	Be, Nb>< Ta (±Sn, B) Beryl- (columbite -tantalite)	low-P, Abukuma amphibolite to upper greeenschist facies (andalusite-sillimanite) ~2–4 kb ~650-500 °C	(interior to marginal to) exterior	quasi-conformable to cross-cutting	Yellowknife field, NWT (Meintzer, 1987); Cat Lake-Winnipeg River field, Manitoba (Černý *et al.*, 1981)
			Beryl -columbite phosphate	Be, Nb > Ta, P (Li, F ± Sn, B) Beryl, columbite-tantalite, triplite, triphylite				
		Complex	Spodumene	Li, Rb, Cs, Be, Ta > Nb (Sn, P, F ± B) spodumene (amblygonite), beryl (lepidolite), tantalite (pollucite)				
			Petalite	Li, Rb, Cs, Be, Ta > Nb (Sn, Ga, P, F ± B) petalite (amblygonite) tantalite, beryl				
			Lepidolite	F, Li, Rb, Cs, Be Ta > Nb (Sn, P ± B) lepidolite microlite beryl, topaz				
			Amblygonite	P, F, Li, Rb, Cs Be, Ta > Nb (Sn ± B) amblygonite (lepidolite), beryl (pollucite), tantalite				
		Albite spodumene		Li (Sn, Be, Ta > Nb ± B				
		Albite		Ta > Nb, Be (Li ± Sn, B)				
	NYF	REE	Allanite - monazite Gadolinite					
Miarolitic				Be, Y, REE, Ti, U, Th, Zr, Nb > Ta, F poor mineralization, gemstock	shallow to sub-volcanic ~1–2 kb	interior to marginal	interior pods and cross-cutting dikes	Pikes Peak, Colorado (Foord, 1982); Korosten pluton, Ukraine (Lazarenko et al., 1973)

observed in nature, particularly in hybrid or mixed-origin pegmatites. Additionally, the distinction between LCT and NYF families, while useful, may oversimplify the spectrum of pegmatite compositions, especially where there is significant overlap or transitional characteristics. Furthermore, some recent classifications, which categorize pegmatites based on their primary accessory minerals and rare-element enrichment, introduce a more detailed perspective yet still require further empirical validation across different geological settings. A critical gap in current classification schemes is their application to field-based studies, where variability in pegmatite formation conditions can be highly localized and influenced by factors not fully accounted for in generalized models. This highlights the need for more flexible, region-specific classification frameworks that can adapt to local geological contexts while still providing a coherent structure for broader comparison.

7. Economic potential of granitic pegmatites

Granitic pegmatites continue to be crucial sources of industrial minerals, coloured gemstones, rare metals, and energy minerals (e.g., Glover et al., 2012; Simmons et al., 2012; London et al., 2012b; London, 2014). Despite industrial minerals such as quartz, feldspar, and mica

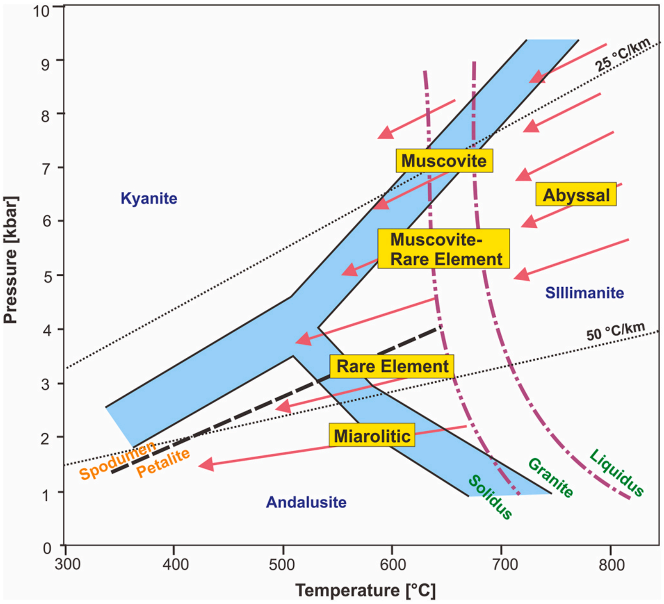

Fig. 3. *P-T* field of environment hosting pegmatite population of the Abyssal (AB), Muscovite (MS), and Rare element (RE) Aluminosilicate boundaries from Robie and Hemingway (1984), cordierite in metapelites after Schreyer and Seifert (1969), Spodumene-petalite from London (1984), granite liquidus-solidus after Jahns (1982), Geothermal gradients from Winkler (1976) (modified after Černý, 1991a).

being found in the majority of rocks commonly as medium to fine grains, the exceptionally coarse grain size of these minerals in granitic pegmatites significantly enhances their economic value up to a potential

Table 7
Typical examples of accessory mineral assemblages in pegmatite groups (after Wise et al., 2022).

Group 1	Group 2	Group 3
Beryl ± columbite ± triphylite ± graftonite	Magnetite ± epidote ± titanite	Andalusite ± sillimanite ± corundum
Beryl ± amblygonite ± columbite	Uraninite ± magnetite	Kyanite ± rutile
Amblygonite ± spodumene	Fayalite ± magnetite	Cordierite ± beryl
Spodumene ± petalite	Arfvedsonite-riebeckite ± fayalite	Sapphirine ± sillimanite
Spodumene ± elbaite	Arfvedsonite-riebeckite ± aegirine ± fluorite	Chrysoberyl ± beryl ± schorl
Spodumene ± lepidolite ± elbaite	Allanite ± gadolinite	Dumortierite ± grandidierite ± borasilite
Spodumene ± albite	Allanite ± monazite ± euxenite	Dumortierite ± schorl
Elbite ± danburite ± hambergite ± zeolites	Allanite + beryl ± columbite	
	Gadolinite ± euxenite ± fergusonite	
	Beryl ± phenakite	
	Microcline (var. amazonite ± fluorite	
	Microcline (var. amazonite ± topaz ± fluorite	

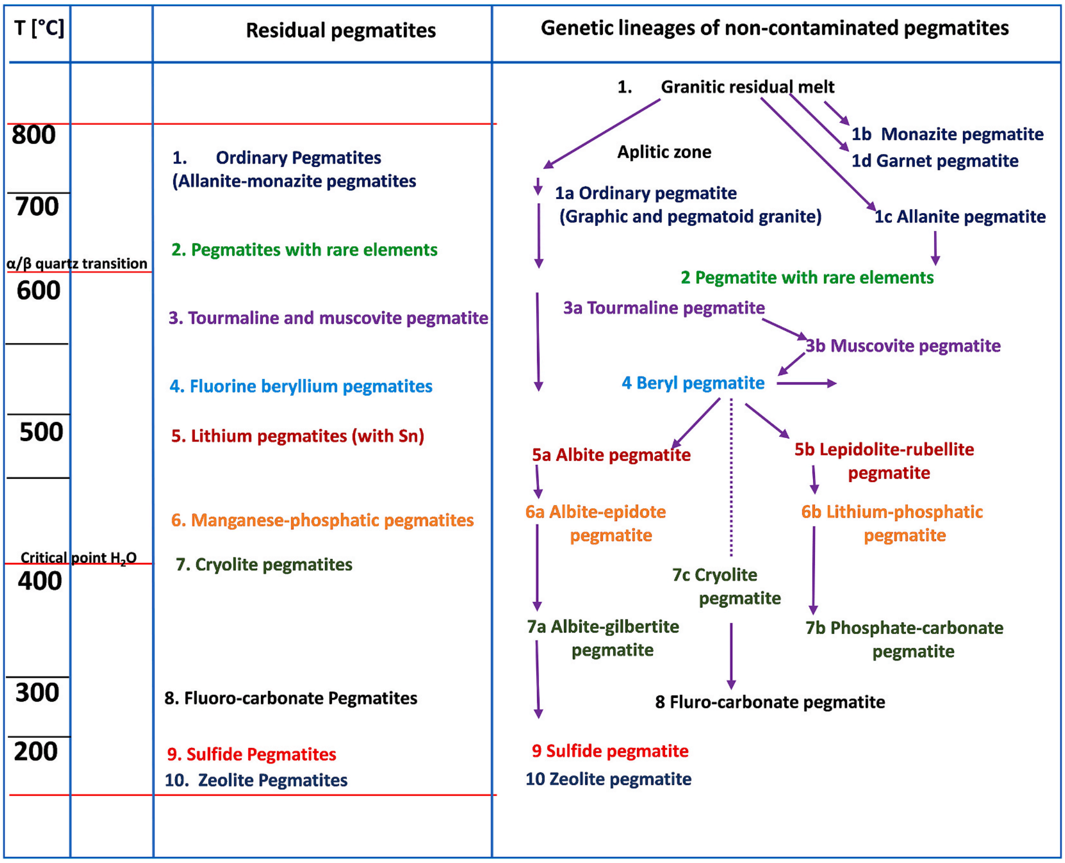

Fig. 4. Classification of ten pegmatitiee phases (residual pegmatites) based on the thermal evolution of pegmatite melt after Fersman (1930). The right column shows the lineage of non-contaminated pegmatite subdividing the 10 thermal phases into 18 pegmatite types modified after Fersman (1967). The Figure modified after Müller et al. (2022).

mining grade. The exotic nature of the pegmatitic melt, enriched with incompatible elements and fluxing components, provides favourable conditions for the crystallization of coloured gemstones, rare metals, and energy minerals, as seen globally.

7.1. As a source of industrial minerals

As granitic pegmatites primarily consist of quartz and feldspars, with some mica-family minerals, certain ore-grade deposits approach almost 100% minable—a rare advantage in the mining industry (London et al., 2012b). On average, pegmatites consist of feldspar (65%), quartz (25%), mica (5–10%, muscovite 6%), and accessory minerals such as spodumene, tourmaline, oxides, garnet, topaz, and muscovite (Kesler et al., 2012; Eagle et al., 2015). Some pegmatites contain kaolin as a secondary mineral, derived from the intense acidic alteration of primary feldspar (Glover et al., 2012). Pegmatites sought primarily for their industrial minerals are referred to as barren, indicating a lack of gems and rare earth elements, and are also known as ceramic pegmatites (Glover et al., 2012).

Various varieties of quartz, such as milky, water-clear, and smoky quartz, are prominent in granitic pegmatites. Quartz is typically purer than other minerals (Glover et al., 2012), although it may sometimes contain Li, Na, K, Ti, and certain impurity minerals (e.g., Müller et al., 2015). Based on purity levels, pegmatitic quartz is divided into two types: high-purity quartz ($<$100 ppm total impurities by weight) (Larsen et al., 2000; Glover et al., 2012), containing less than 50 ppm trace element concentration (Harben, 2002), and low concentrations of elements other than silicon and oxygen ($>$99.995% SiO_2) (Larsen et al., 2000; Müller et al., 2015). However, a few pegmatite bodies contain quartz pure enough to produce high-purity quartz powder [High-purity quartz powder is produced from pegmatites in Brazil, India, Australia, Madagascar, Norway, China, the USA, and Russia (Glover et al., 2012)]. The chemistry of pegmatite quartz is mainly controlled by the origin (chemistry of the source rock) of pegmatitic melts and, occasionally, the geodynamic setting of the pegmatite fields and provinces (Müller et al., 2021).

Albite and microcline are common feldspar varieties found in ceramic pegmatites. These alkali-feldspars crystallize over extensive periods of pegmatite solidification and serve as suitable hosts for Rb, Cs, Ca, Sr, Pb, Ba, Eu, La, and Li in the alkali position, and B, Ga, Ge, Fe, Mg, Ti, and P in tetrahedral sites (Oyarzábal et al., 2009). The different feldspar types have various applications related to their melting temperature and are used in various industries according to specific requirements.

Kaolin deposits and occurrences could be primary or secondary depending on their genesis (Bailey, 1980; Dixon, 1989; Murray, 1999; Ekosse, 2010). Primary deposits form due to the alteration of crystalline rocks, while secondary deposits result from the erosion of primary deposits (Prasad et al., 1991). Most kaolinite deposits form as a consequence of hydrothermal leaching or weathering of feldspars. Additionally, acid leaching helps remove ions such as calcium, sodium, and potassium, resulting in the production of kaolin or kaolinite (Glover et al., 2012).

7.2. As a source of strategic metals

Strategic metals, pose the greatest risk of supply disruptions globally and play a vital role in a country's economy or defense (Linnen et al., 2012). The availability of strategic metals varies from country to country, with key metals including Li, Ta, Nb, Be, Sb, W, Co, and rare earth elements. These metals are commonly found in rare-element pegmatites, which are mineralogically complex and enriched with incompatible elements (Černý, 1991a; Simmons and Webber, 2008; Linnen et al., 2012; Bradley et a; Rosing-Schow et al., 2023). Notably, many of these incompatible elements align with strategic metals (Linnen et al., 2012; Hulsbosch et al., 2014).

During the initial stages of the crystallization process, quartz and feldspar dominate. Because strategic metals are highly incompatible with these minerals, their concentrations in residual melts experience a significant increase. For example, cesium (Cs) as a highly incompatible element due to its larger ionic radius, except in mica, feldspar, and cordierite, where it is moderately incompatible (London, 2005). Rubidium is also an incompatible element but is compatible with mica and alkali feldspar. Beryllium is normally incompatible due to its small ionic radius but is compatible with cordierite and muscovite (Linnen et al., 2012). This type of pegmatite also contains minerals with Li, Nb, W, Cs, and Be, which are by-products of tin- and tantalum-pegmatite mining (Sweetapple and Collins, 2002).

The most granitic pegmatites containing quartz and feldspar have a low concentration of rare-earth elements (Stilling et al., 2006; Linnen et al., 2012). Rare-earth element pegmatites make up only 1%–2% of all pegmatites (London, 2014). They consist of elements such as Be, Li (spodumene and petalite), Sn (cassiterite), Rb (lepidolite), Ta and Nb (Ta-oxide minerals), Cs (pollucite), REEs, and U, which may be highly enriched in pegmatites compared to the bulk continental crust. Some enrichment factors (relative to the continental crust) exceed 10,000 to 100,000 (Galeschuk and Vanstone, 2007; Černý, 1991a; Černý and Ercit, 2005). These are typically found in geographically restricted areas, along large regional-scale faults in greenschist and amphibolite facies metamorphic terrains (Selway et al., 2005). The rare-element-rich granitic pegmatites represent the youngest, most fractionated end-members of layered sequences in upwardly differentiated plutons (Černý et al., 2005; Linnen and Cuney, 2005; Melcher et al., 2015). Additionally, rare-element pegmatites contain fluxing compounds, which lower the viscosity and solidus temperature of the magma (Suwimonprecha et al., 1995; Melcher et al., 2015). Consequently, crystal-melt fractionation and the concentration of rare metals occur in residual melts, aided by liquid-liquid separation and fluid separation at the magmatic-hydrothermal transition (Černý et al., 2005; Melcher et al., 2015).

The geochemical signatures of rare-element pegmatites are particularly intriguing as they represent the extremes of fractionation trends encountered in the final stages of magmatic differentiation, found in very leucocratic, high-silica, metaluminous to peraluminous granites, and rhyolites (Černý and Ercit, 1985). Rare earth, which represents LCT and NYF pegmatites, hosts several strategic metals (Černý, 1991a).

7.2.1. LCT pegmatites as a source of strategic metals

LCT (Lithium-Cesium-Tantalum) pegmatites are of significant importance in industrial applications (Melcher et al., 2015), encompassing elements such as Li, Cs, Ta, and Be, tantalum oxide, Be, B, F, P, Mn, Ga, Rb, Nb, Sn, and Hf, as well as ceramic-grade feldspar and quartz (London, 2017; Goodenough et al., 2019). LCT pegmatites are characterized by a high K/Na ratio, low Ca and Na content, high Al content, and a low oxidation state (Selway et al., 2005). Consequently, these pegmatites typically exhibit the presence of biotite and muscovite, while lacking hornblende (Selway et al., 2005). The LCT pegmatites as crystallized from magma resulting from the partial melting of preexisting sedimentary source rocks (Shelley, 1993; Selway et al., 2005).

Presently, most authors believe that LCT family pegmatites originate from S-type (Černý et al., 2012) peraluminous [Al-rich $Al/(Na + K + 2Ca) > 1$], quartz-rich granites associated with the melting of schists and gneisses of sedimentary origin (Černý et al., 2012; London, 2017). S-type granites typically form in areas with crustal thickening and are associated with subduction and continental collision. Additionally, LCT pegmatites are believed to be derived in syntectonic areas, as the sources of these granitic pegmatites lack foliation or pervasive deformation (Černý et al., 2012).

LCT pegmatites play a crucial role in supplying rare and strategic elements globally, contributing to one-third of the world's lithium production, most of the tantalum, and the entire world's cesium requirements (Geological Survey of the U.S., 2011). These pegmatites host various rare-element-bearing mineral phases, including beryl, spodumene, elbaite, columbite-tantalite, pollucite, and lithium phosphates (Dwight and Andrew, 2013). Dwight and Andrew (2013) estimated millions of tonnes (Mt) of ore, with indicated percentages of tantalum and lithium oxides (Ta_2O_5 and Li_2O), from larger scale deposits such as Tanco in Canada (2.1 Mt at 0.215 percent Ta_2O_5), Greenbushes in Australia (70.4 Mt at 2.6 percent Li_2O), and Bikita in Zimbabwe (12 Mt at 1.4 percent Li_2O).

7.2.2. NYF pegmatites as a source of strategic metals

NYF (Niobium-Yttrium-Fluorine) pegmatites encompass the rare-element-REE and miarolitic-REE subclasses (Selway et al., 2005) and are enriched with Nb, Y, F and occasionally contain economic resources of these metals (Goodenough et al., 2019; Eby, 1990; Černý and Ercit, 2005; Martin and De Vito, 2005; Simmons and Webber, 2008). These pegmatites are derived from A- and I- type granites (Černý and Ercit, 2005; Martin and De Vito, 2005). The A-type of granites, which are subaluminous to metaluminous (Černý, 1991a; Selway et al., 2005), can be found in the lower crust but vary with the amount of added mantle components (King et al., 1997; Christiansen et al., 2007). The NYF-type granitic pegmatites form during peralkaline igneous rocks that fractionate directly from mantle sources. This type of granite has high K + Na, F, and Zr, low Al and Ca, and high Fe/Mg (Martin and De Vito, 2005; Selway et al., 2005), characterized by the presence of Fe-rich mica, pyroxene, and amphiboles (Selway et al., 2005). This family contains chemically complex oxides and silicates carrying heavy elements Ti, U, Th, and Nb over Ta, including minerals such as euxenite/aeschynite [$(Y,Ca,Ce,U,Th)(Nb,Ta,Ti)_2O_6$], allanite-(Y) [$CaYFe^{2+}Al_2Si_3O_{12}(OH)$], samarskite/fergusonite [$(Y,Fe^{3+},Fe^{2+},U,Th,Ca)(Nb,Ta)O_4$], and gadolinite [$(Y,Ca)_2Fe^{3+}Be_2Si_2O_{10}$] (Černý et al., 2012). Abundant fluorite or topaz in NYF pegmatites reflects their enrichment in fluorine (Černý et al., 2012).

7.3. As a source of gem-bearing minerals

All significant gem-bearing pegmatites share a granitic composition (Keller, 1990; Simmons et al., 2012), hosting more than 50 familiar gemstones occurring in various oxide, phosphate, and silicate minerals (London, 2008). Granitic pegmatites are vital sources for coloured gemstones such as tourmaline, topaz, spessartine polychrome, various coloured varieties of beryl like aquamarine, emerald, morganite, amazonite, the green variety of microcline, and coloured spodumene crystals like kunzite and hiddenites (Pezzotta and Laurs, 2011; Simmons et al., 2012; Hickman, 1983; Sweetapple and Collins, 2002). Although gem crystals are typically smaller than industrial minerals like quartz and feldspar, exceptional cases with larger gem-quality crystals like topaz, aquamarine, and tourmaline extending to several meters have been recorded (Keller, 1990). Minas Gerais, Brazil, is renowned for large crystal findings, including the largest aquamarine crystal (110.5 kg) discovered in 1910 at the Papamal mine (Keller, 1990). Table 8 summarizes the major gem-pegmatite districts and notable gem minerals in the world.

While gemstone pegmatites primarily originate in-situ, secondary gem pockets formed during transportation and erosion are also observed (Proctor, 1985). Brazil is particularly famous for gem-bearing pegmatites, with notable finds of blue-green, blue, and red tourmaline (Proctor, 1985). The Olhod'Água mine and Aracuai-Itinga district mining are well-known locations for gem-bearing pegmatites in the Eastern Brazilian pegmatite province (Proctor, 1985).

Sri Lanka, with its high abundance of gemstones, often associated with high-grade metamorphic rocks like granitic gneiss and pegmatites, is another significant source. Studies (e.g., Herath, 1985, 1985; Munasinghe and Dissanayake, 1980) suggest that the source of precious gem varieties found in gem gravels in Sri Lanka are likely pegmatite. Central Madagascar is also characterized by the presence of gem-bearing pegmatites (Pezzotta, 2001, 2005). Some gem minerals (e.g., tourmaline group minerals, beryl group minerals, spessartine) are more frequently hosted in granitic pegmatites than in other rock types. Cornwall, United Kingdom, and Phuket, Thailand are renowned localities for gem-quality tourmaline-bearing pegmatites (Suwimonprecha et al., 1995). Boron, an incompatible trace element, can be highly enriched in granitic melts and aqueous fluids, facilitating the crystallization of the tourmaline group minerals. The Beryl group contains various gem varieties because many ions can substitute the beryl crystallographic structure (McManus et al., 2008). Gem-quality beryl varieties like Aquamarine, Emerald, and Goshenite are found in well-known localities such as Sparrow Pluton (Yellowknife, NWT, Canada) and Helen Beryl Black Hills, USA (Abduriyim et al., 2006; Simmons et al., 2012). Spessartine, a gem-quality garnet variety, can be found in some pegmatites, with famous localities like Alto Mirador pegmatite, Escondido pegmatite, and Poaiá pegmatites in Brazil (Eeckhout et al., 2002). Ramona, California, is also renowned for spessartine gem-bearing pegmatites.

Table 8
Major gem-pegmatite districts and notable gem minerals in the world.

Pegmatite/pegmatite field and the country	Notable gem minerals
Minas Gerais in Brazil	Beryl (aquamarine, morganite, heliodor), topaz, tourmaline, spodumene (kunzite, hiddenite), brazilianite, euclase, quartz (rose, smoky, citrine), amblygonite–montebrasite
Paraíba, Rio Grande do Norte in Brazil	Tourmaline (Paraíba variety), beryl (aquamarine, morganite, heliodor), euclase, quartz (rose, smoky, citrine), spessartine
Central and Eastern Zambia	Tourmaline, beryl (emerald), spessartine
Katanga, Nord Kivu, D. R. Congo:	Tourmaline
Coast in Kenya	Tourmaline
Erongo in Namibia	Tourmaline, beryl (aquamarine), topaz, jeremejevite
Edo, Kaduna, Kwara, Nassarawa, Oyo, Plateau in Nigeria	Tourmaline, chrysoberyl, topaz, beryl, phenakite, spodumene, spessartine
Mashonaland West, Zimbabwe	Beryl (aquamarine), topaz, tourmaline
Nampula, Tete, Zambezia in Mozambique	Tourmaline, spessartine, beryl (aquamarine), topaz, spodumene (kunzite), quartz (rose)
Matale, Awissawella, Balangoda, Meetiyagoda in Sri Lanka	Saphire, amazonite, topaz, moonstones
Arusha, Morogoro, Tanga in Tanzania:	Tourmaline, spessartine
Antananarivo, Fianarantsoa, Toamasina in Madagascar	Tourmaline, beryl (aquamarine), spodumene (kunzite), londonite, pezzottaite, hambergite, orthoclase/sanidine, quartz (rose), spessartine, danburite, phenakite
California, Mesa Grande, Pala, Ramona in United States	Tourmaline, beryl (aquamarine, morganite), spessartine, spodumene (kunzite)
Colorado Collegiate Range in the United States	Beryl (aquamarine), phenakite
New England, Maine, New Hampshire, and Connecticut in the United States	Tourmaline, beryl (aquamarine), pollucite
Zhytomyr in Ukraine	Beryl (heliodor, aquamarine), topaz
Ural Mountains in Russia	Beryl (aquamarine, emerald), topaz, chrysoberyl (alexandrite)
Zabaykalsky (Transbaikalia) in Russia	Tourmaline, danburite, pollucite, spessartine, beryl (aquamarine), topaz
Elba in Italy	Tourmaline, pollucite
Luumäki (South Karelia) in Finland	Beryl (aquamarine), tourmaline
Mogok, Momeik in Myanmar	Tourmaline, phenakite, petalite, pollucite
Yen Bai in Vietnam	Tourmaline, microcline (amazonite)
Xinjiang Uygur in China	Beryl (aquamarine), tourmaline
Yunan in China	Tourmaline, beryl (aquamarine), spessartine
Tamil Nadu in India	Beryl (aquamarine)
Kunar, Nuristan in Afghanistan	Tourmaline, spessartine, topaz, beryl (emerald, aquamarine), spodumene (kunzite)
Gilgit-Baltistan in Pakistan	Tourmaline, spessartine, beryl (aquamarine), topaz

Sources: Pezzotta (2001); Falster et al. (2001, 2005); Groat et al. (2007); Simmons (2007); Cornejo and Bartorelli (2010); Shigley et al. (2010); Clifford (2012), Dharmapriya et al. (2020)

7.3.1. *Origin of gem-forming melts*

Gem minerals are believed to form in pegmatites from rare elements that cannot be incorporated into the crystal structure of initially crystallized minerals like quartz, feldspar, and mica (Keller, 1990). Most gem-quality minerals originate during the final stages of the crystallization of a parent granitic melt (Simmons et al., 2012). The pegmatite-forming melts with the potential for crystallizing gem minerals mostly originate during the crystallization of a parental granitic melt (Simmons et al., 2012). During the fractional crystallization of magma, if the concentration of volatiles, mainly H_2O, exceeds its solubility limit in the remaining residual melt, an aqueous fluid exsolves from the melt, promoting the formation of a miarole or some primary pockets (e.g., Simmons et al., 2012). Keller (1990) points out that the abundance of hydrous minerals, including clays and zeolites, together with gem-quality minerals in pockets in Gem Pegmatites of Minas Gerais, Brazil, serves as evidence of the role of fluid in the final stages of crystallization. Sometimes gem-quality minerals intergrow with feldspar, quartz, and mica. Corundum is poorly associated with quartz but predominantly occurs in feldspars. The exact mechanism for the formation of these unusual melts of pegmatites is still unclear. One hypothesis suggests that these unusual pegmatites were stripped off silica from the surrounding rocks, allowing the formation of corundum. Rare gem varieties sometimes occur at the contact between the pegmatite body and its host rocks, interpreted as open system formation due to metasomatism (Schwarz et al., 2002; Zwaan et al., 2005; Groat et al., 2007; Keller, 1990).

7.3.2. *Relations with occurrences of gem-quality minerals in relation to pegmatite anatomy*

Gemstones typically constitute only a small fraction of pegmatite bodies (Shigley et al., 1984). Gem-quality minerals are primarily found in the interiors of zoned pegmatites or reaction zones adjacent to pegmatites and host rocks. Three main settings within pegmatites where gemstones are commonly found have been summarized by Simmons et al. (2012): (i) *Setting 1*: Crystals "frozen" in massive quartz or feldspar in the core or margin of the core of a pegmatite: This setting includes minerals such as aquamarine and tourmaline in massive quartz or feldspar, usually with only parts of these crystals occurring as gem-quality. (ii) *Setting 2*: Crystals in reaction zones surrounding pegmatites that intrude mafic rocks: These crystals are produced from the interaction of Be-rich pegmatitic fluids with chromium-bearing mafic country rocks. Examples include alexandrite and emerald found in the Ural Mountains of Russia, the Mananjary area of Madagascar, and the Kafubu area of Zambia. (iii) *Setting 3*: Crystals in miarolitic cavities (pockets): Miarolitic cavities are crystal-lined voids or crystal-filled and clay-packed masses within igneous hosts. These pockets, comprising about 5% of the total pegmatite volume, contain gem-quality minerals. Factors influencing minerals precipitated in these cavities include source rock composition, the amount and composition of volatiles present, and pressure and temperature conditions during melt solidification. Gem varieties such as beryl, spessartine, spodumene, topaz, and tourmaline can occasionally be found in miarolitic cavities, along with minerals like kaolin, smectite, chlorite, oxides, carbonates, and other phyllosilicate group minerals.

The size of miarolitic cavities varies, and examples from around the world include gem pockets in the Dunton pegmatite on Newry Mountain, Maine, USA (up to 2 × 3 × 7 m sizes) containing bicolored, green, and red elbaite tourmaline crystals, and gem pockets in the Mount Mica pegmatite in Maine, USA (1.5 × 2 × 7 m sizes) producing large tourmaline crystals. Notable gem pockets are also found in the Jonas pegmatite (Conselheiro Pena district of Brazil), Volodarsk-Volynsky, Ukraine, and various other locations globally. Fig. 5 represents a flow chart summarizing the development of gem quality crystals in miaroles in pegmatite. Fig. 6 is a schematic diagram showing a cross-section through a pegmatite with gem pockets (modified after Gadas et al., 2012).

7.4. *As a source of energy minerals*

The identification of energy minerals is crucial for environmental stewardship, human health, and sustainable growth (Ferrero et al., 2013). Uranium and thorium, characteristic energy minerals, are often

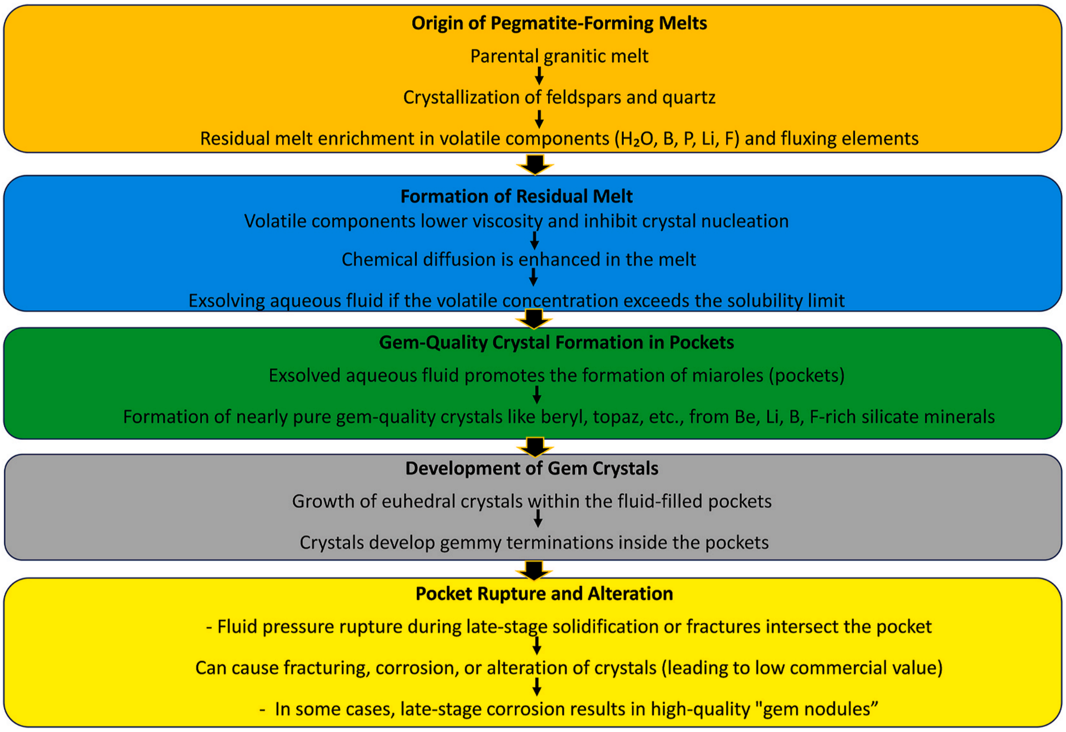

Fig. 5. A flow chart summarizing the development of gem-quality crystals in miaroles in pegmatite.

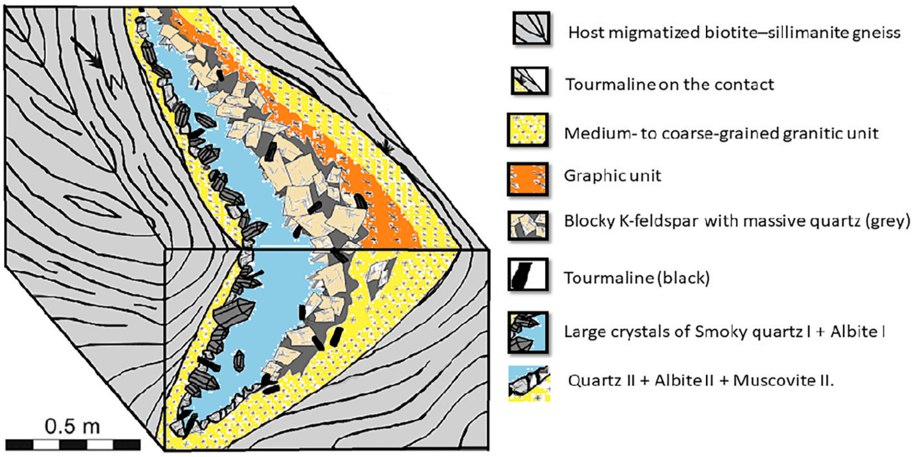

Fig. 6. A schematic diagram showing an across-section through a pegmatite with gem pockets (modified after Gadas et al., 2012). Labeling after Gadas et al. (2012). Different mineral assemblages on the hanging-wall part (large crystals of smoky quartz I up to 25 cm long + albite I) and the footwall part of the pocket (large corroded crystals of K-feldspar up to 30 cm in size muscovite II + subparallel crystals of smoky quartz II + tourmaline).

present in igneous rocks as part of the late-stage differentiation of granite or syenite (Virk and Singh, 1977). Besides industrial minerals, strategic metal-bearing minerals, and gemstones, certain pegmatites contain high levels of U- and Th-bearing minerals like uraninite and thorianite, are serving as potential sources of nuclear energy (Dill, 2015).

Uranium minerals in pegmatites can be categorized as primary and secondary based on their origin. Primary uranium minerals include simple oxides, multiple oxides (columbium, tantalum, and titanium), miscellaneous compounds, and carbonaceous material. Most primary uranium minerals undergo partial or complete alteration to secondary minerals such as hydrated oxides, phosphates, arsenates, sulfates, silicates, and carbonates (Tyler, 1950; Nete, 2009). Examples of uranium mineralization in pegmatites include uraninite, uranophane, beta-uranophane, and uraniferous pyrochlore. In some instances, uranium occurs as small grains embedded with mica flakes or garnet grains.

Significant uranium deposits in Gascoyne Province, South Africa, demonstrate pegmatites and aplite containing disseminated uraninite betafite and secondary uranium minerals (Berning et al., 1976). Madagascar is also renowned for uranium-bearing pegmatites, with locations like Ambatofotsy, Abatohasana, and Ambatofampykely containing large pegmatites averaging 12%–15% U_3O_8 (Bourret, 1988). Studies on the Guangzhou uranium deposit in China reveal the enrichment of uraninite hosted in granitic pegmatites, occurring commonly as mineral inclusions in quartz, K-feldspar, and biotite. Post-tectonic magmatism and hydrothermal activities are suggested to contribute to the remobilization and circulation of uranium into pegmatites (Wu et al., 2021).

8. Tectonic settings of granitic pegmatites

The global distribution of pegmatite ages implies a connection between the age of pegmatite formation and supercontinent assembly (Bradley, 2011; Bradley et al., 2017). Bradley et al. (2017) highlighted the correlation of LCT (Lithium-Cesium-Tantalum) pegmatite age distribution with supercontinent assembly throughout geological history. According to the authors, pegmatite ages from the Appalachians in North America and the Hercynides and Uralides in Eurasia, ranging from 370 to 275 million years ago (Ma), signify collisional events during the assembly of Pangea. Overlapping peaks at 530 and 485 Ma in pegmatites from Brazil, Australia, India, Namibia, and Ethiopia coincide with the assembly of Gondwana. In the Precambrian, LCT pegmatites globally exhibited peaks at 960 Ma, 1800 Ma, and 2650 Ma, corresponding to the assembly of Rodinia, Nuna, and Superia supercontinents, respectively. Subduction of oceanic crust and continental-continental collision associated with supercontinent amalgamation provides favourable conditions for the formation of large igneous provinces (Klausen, 2020).

Tkachev (2011) noted that the occurrence of continental granitic magmatism and the emplacement of LCT pegmatites followed a consistent cycle of about 800 million years. Significant peaks in the global age distribution of LCT pegmatite fields were observed at 2650–2600 Ma, 1900–1850 Ma, 1000–950 Ma, and 300–250 Ma (Fig. 7). Tkachev (2011) also identified additional peaks at 2850–2800 Ma, 2100–2050 Ma, 1200–1150 Ma, and 550–500 Ma. These periods correspond with heightened continental crust magmatism and align well with Bradley's (2011) proposed supercontinent cycles. While continental crust magmatism dates back to 3850 Ma, no LCT pegmatites have been recorded prior to around 3150 Ma (Fig. 7). Each period of increased LCT pegmatite emplacement lasted approximately 50 million years.

Martin and De Vito (2005) extended the tectonic classification of granite magmatism to the field of granitic pegmatites. According to Martin and De Vito (2005), LCT granitic pegmatites are part of orogenic suites associated with crustal shortening, occurring in zones of subduction and instances of continental collision. The parental magma is derived by partial melting in the mantle wedge within a tectonic environment characterized by overall compression, extending from the upper mantle to the lower crust, experiencing assimilation and fractional crystallization. Magma upwelling facilitates the partial melting of

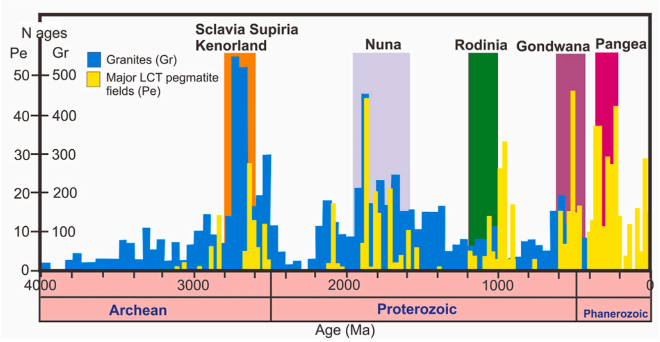

Fig. 7. Age distribution patterns of significant LCT (Lithium-Cesium-Tantalum) pegmatite fields and associated granites (Pe and Gr) based on data from Condie et al. (2009) and McCauley and Bradley (2014). The age distributions of major LCT pegmatite fields are derived from Tkachev (2011). Coloured bars indicating the estimated assembly periods of supercontinents. The figure is modified after Dittrich et al. (2019).

muscovite- and biotite-bearing metasedimentary sequences of the crust, resulting in contrasting magmas juxtaposed due to magma mixing and mingling. The extreme fractional crystallization of these magmas produces metaluminous to peraluminous granitic pegmatites involving both crust and mantle source materials to varying extents. Bradley (2019) noted the lack of a comprehensive study addressing the detailed plate tectonic settings of LCT pegmatites. However, they may form in possible tectonic settings involving partial melting of the continental crust, such as (a) subduction beneath a continental-margin arc; (b) slab failure (breakoff, delamination, or rollback) during or after collision; (c) overthickening of continental crust during collision, including variants involving shear heating and radiogenic heating; (d) extensional collapse during or after collision; and (5) rise of a mantle "plume" below a recently formed orogenic belt (Bradley, 2019). Bradley et al. (2017) argued that the 7 Ma LCT pegmatites in Elba Island, Italy formed through a combination of (b) and (d) when slab rollback during the Apennine collision caused the mantle to well up and partially melt beneath an extending collisional orogeny.

According to Martin and De Vito (2005), NYF (Niobium-Yttrium--Fluorine) pegmatites are interpreted as products of anorogenic suites and mainly form in an extensional setting. These pegmatites represent the culmination of protracted fractional crystallization of basaltic

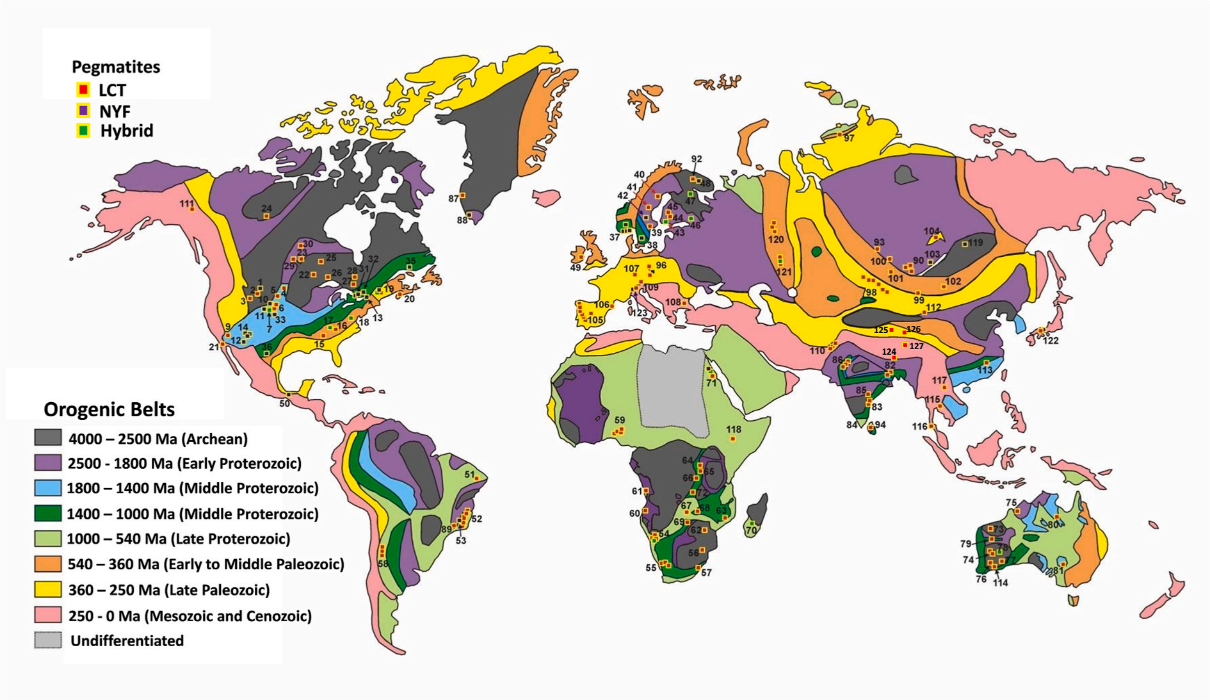

Fig. 8. Map of the world showing the geological distribution of 127 pegmatite provinces and districts, distinguishing between LCT (Lithium-Cesium-Tantalum) and NYF (Niobium-Yttrium-Fluorine) suites, as well as some with hybrid affiliations. The map of orogenic belts is based on Utsunomiya et al. (2007) and Rino et al. (2008). Legend: 1. Bighorn Mt. (WY, USA); 2. Copper Mt. (WY, USA); 3. South Pass (WY, USA); 4. Black Hills (SD, USA); 5. Haystack Range (WY, USA); 6. Routt Plutonic Suite (CO, USA); 7. Trout Creek Pass (CO, USA); 8. White Picacho (AZ, USA); 9. Mohave Co (AZ, USA); 10. Laramie Mt (WY, USA); 11. Berthoud Plutonic Suite (CO, USA); 12. Burro Mtn (NM, USA); 13. Adirondack Highlands (NY, USA); 14. North New Mexico fields (USA); 15. Rockford (AL, USA); 16. Kings Mountain (NC, USA); 17. Spruce Pine (NC, USA); 18. Amelia (VA, USA); 19. New England districts (USA); 20. Brazil Lake (Nova Scotia, Canada); 21. Southern California (USA); 22. Cat Lake – Winnipeg River (Manitoba, Canada); 23. Wekusko Lake (Manitoba, Canada); 24. Yellowknife Basin (NW Territories, Canada); 25. NW Ontario fields (Canada); 26. Superior Lake (ON, Canada); 27. Lac Simard (QC, Canada); 28. Preissac – Lacorne (QC, Canada); 29. Birch Portage – Hanson Lake (SK, Canada); 30. Granville Lake (Manitoba, Canada); 31. SW Grenville southern fields (ON, Canada); 32. SW Grenville northern fields (ON, Canada); 33. Mt Laurier and Gatineau fields (QC, Canada); 34. Lac Turgeon – Johan Beetz (QC, Canada); 35. Pikes Peak (CO, USA); 36. Llano-Burnet (TX, USA); 37–38. Sveconorwegian Province in S Norway and SW Sweden (Evje-Iveland, Froland, Glamsland, Arendal, Søndeled, Kragerø, Tørdal, Østfold-Halland); 39. Uttö-Mysingen (Sweden); 40. Varuträsk (Sweden); 41. Bothnian Basin (Sweden); 42. Falun (Central Sweden); 43. Kemiö – Orijärvi (Finland); 44. Eräjärvi (Finland); 45. Seinäjoki (Finland); 46. Ladoga Lake (Russia-Finland); 47. Chupa-Ijona (Karelia, Russia); 48. Keivy Massif, Kola Peninsula (Russia); 49. Leinster (Ireland); 50. El Muerto pegmatites (Oaxacan Complex, Southern Mexico); 51. Borborema Province (RGN, PB, Brazil); 52. Eastern Brazilian Province (MG, BA, ES, Brazil); 53. Sta Maria de Itabira (MG, Brazil); 54. Damara Province (Namibia); 55. Namaqualand (South Africa); 56. Kaapvaal (South Africa); 57. Natal districts (South Africa); 58. Panpean Pegmatite Province; 59. SW Nigeria Province (Ago-Iwoye, Keffi, Nassarawa, Komu, Wamba districts); 60. Giraul (SW Angola); 61. Caxito (NW Angola); 62. Bikita (Zimbabwe); 63. Alto Ligonha (Mozambique); 64. Ruanda; 65. Burundi; 66. Kobokobo, Kamituga area, South Kivu (Congo); 67. Kapiri Mposhi (Zambia); 68. Lundazi (Zambia); 69. Choma-Kalomo (Zambia) and Kamativi (Zimbabwe); 70. Itremo (Madagascar); 71. Southeastern Desert Province (Egypt); 72. Manono-Kittolo (Shaba, Congo); 73. Pilbara (WA, Australia); 74. Lake Moore - Dalgaranda (WA); 75. King Leopold (WA); 76. Greenbushes (WA); 77. Coolgardie – Norseman (WA); 78. Mukinbudin (WA); 79. Gascoyne (WA); 80. Mt. Isa (QNL); 81. Olary and Broken Hill, Curnamona Province (SA-NSW); 82. Bihar Mica Belt (India); 83. Nellore Mica Belt (India); 84. Tamil Nadu Belt (India); 85. Bastar-Malkagiri Belt (India); 86. Rajasthan Belt (India); 87. Nuuk Region (Greenland); 88. Gardar Province (Greenland); 89. Volta Grande, Sao Joao de Rei (Brazil); 90. Strange Lake (Labrador, Canada); 91. Alakha (Russia); 92. Kolmozero-Voronya (Kola Peninsula, Russia); 93. Yenisei Ridge (Russia); 94. Highland Complex (Sri Lanka); 95. Ghaha-Cote d'Ivoire; 96. Bohemian-Moldanubicum Belt; 97. Taimyr Fold Belt (Russia); 98. Altai Belt (China, Kazakhstan, Russia); 99. Mongol-Okhotsk Fold Belt; 100. East Sayan Mt. (Siberia, Russia); 101. Southern Tuva (Kamar-Daba Fold Belt); 102. East Transbaikalia (Russia); 103. NW Baikal (Russia); 104. Mama-Chuya, North Baikal Highland (Russia); 105. Iberian Peninsula; 106. Creus Cap (Spain); 107. Hagendorf-Pleystein (Babaria, Germany); 108. Paranesti (NE Greece); 109. Koralpe (Austria); 110. Afghanistan-Pakistan Belt; 111. Little Nahanni (NW Territories, Canada); 112. Jiajika, Kangdi (Sichuan Province, China); 113. Nanping (China); 114. Cattlin Creek – Cocanarup, Ravensthorpe (WA); 115. Tak (Thailand); 116. Phuket (Thailand); 117. Lao Cai and Phu Tho (Northern Vietnam); 118. Kenticha (Ethiopia); 119. Nimnyr Block, Central Aldan (Russia); 120. Middle Urals (Russia); 121. South Urals (Russia); 122. Southern Japan (Japan); 123. Central Alps; 124. Qiongjiagang in Tibet; 125. Heiyingshan in Xinjiang (China); 126. Jing'erquan in Xinjiang (China), 127. Chaka in Qinghai (China).

magma. Crustal extension occurs above zones of anomalous upper mantle and active degassing, producing a mixture of H_2O, CO_2, and CH_4. Trace elements, including alkalis, rare earths, Nb, Ta, Zr, Ti, U, and Th, are mobilized upward into the attenuated crust. The lower and middle crusts are locally alkali-metasomatized before anatexis. Crustal anatexis produces a metaluminous to mildly peralkaline melt. Simultaneously, the rising mantle-derived Oceanic Island Basalt-type magma promotes the progress of anatexis. The uncontaminated basaltic magma may fractionate in a classic way or mix with derivative magmas through the partial melting of the metasomatized crust. The final product may be an NYF-type pegmatite. However, recent investigations (Müller et al., 2017) concluded that NYF pegmatites are not necessarily formed in an anorogenic tectonic setting in relation to A-type magmatism. They can result from both compressional or extensional orogenic settings unrelated to pluton-scale magmatism.

The tectonic settings of "Mixed" type (LCT + NYF) pegmatites have received little attention throughout history. Several authors (e.g., Černý, 1991b) have pointed out the association of LCT pegmatites with S-type granites (Chappell and White, 1992) and NYF pegmatites with A-type granites (Eby, 1990). Both these granite types are tectonically controlled, with A-types associated with extensional rift environments within continental cratons and S-types associated with the melting of accreted marine sediments in the waning stages of continental collisions (London, 2022). One possible tectonic environment where these two contrasting granite magma types might arise in close association is in the back-arc basins behind subduction-related volcanic arcs that extend into continental margins to produce mixed-type pegmatite (London, 2022).

Fig. 8 represents the geological distribution of 127 pegmatite provinces and districts, distinguishing between LCT and NYF suites and some with hybrid affiliation mainly after Sánchez-Muñoz et al. (2017) and some from Li et al. (2023). These regions are predominantly associated with orogenic belts linked to crustal convergence, indicating a compressional tectonic regime. However, granitic pegmatites can also form in tectonically stable environments, signifying an extensional regime. Most large, mineralized pegmatites are found in collisional orogens, within districts containing numerous individual pegmatitic bodies. Such extensive pegmatite fields are generally absent in non-collisional settings, such as the western part of the American continent and the eastern part of Australia, due to the lack of thickened continental crust required to generate the necessary heat and pressure for melt formation (Tkachev, 2011; Sánchez-Muñoz et al., 2017).

Current research has advanced our understanding of pegmatite formation, yet the variability in tectonic settings—especially the role of specific processes like slab rollback, mantle plumes, and extensional collapse—remains an area for further exploration. Understanding these tectonic drivers in greater detail could provide further deeper insights into the conditions necessary for the emplacement of economically significant pegmatite bodies. Therefore, future studies should aim to refine these models, taking into account of regional geological context and integrating multidisciplinary data to better predict pegmatite occurrences and their mineralization potential.

9. Summary

Granitic pegmatites are a widespread rock type characterized by a granitic composition, representing chemical compositions of $NaAlSi_3O_8$–$KAlSi_3O_8$–Al_2O_3–SiO_2 (London et al., 2012a). This rock type is texturally distinctive due to large crystals and is often marked by zonation, reflecting variations in grain size, mineral assemblage, crystal habit, or rock fabric. Most granitic pegmatites usually contain quartz, feldspar, mica, and over about fifty accessory mineral species (Bastin, 1910, 1911) including secondary minerals and rare earth elements.

During the crystallization of felsic magma, quartz and feldspar minerals become enriched in the residual melt. Concurrently, the content of rare earth elements, exotic components, and volatile components increases. These compositions are excluded in the initial crystallization of quartz and feldspar, leading to a residual melt eventually saturated in minerals containing these exotic components. Granitic pegmatites, therefore, exhibit high concentrations of various elements, including Li, Rb, Cs, Be, Ga, Sc, Y, REE, Sn, Nb, Ta, U, Th, Zr, and Hf, typically present at trace levels. Fractional crystallization may further enrich these elements in pegmatites up to higher levels, typically observable in few wight percentages (London, 2008; Fredriksson, 2017).

The strategic elements present in granitic pegmatites are a few thousand times higher than their crustal abundance (Černý, 1991a; Simmons and Webber, 2008; Linnen et al., 2012; Bradley et al., 2017). This enrichment of exotic chemical constituents facilitates the crystallization of economic commodities such as strategic metal enriched-minerals, precious and semiprecious gemstones, and energy minerals. However, rare element-enriched pegmatites are rare in nature, and the majority of pegmatites contain only industrial minerals, often referred to as barren or ceramic pegmatite.

Three main hypotheses propose the formation of pegmatites: (i) Fractional crystallization, (ii) direct formation by anatexis of surrounding rocks, typically in the presence of fluids, and (iii) Liquid immiscibility. Recent studies suggest that granitic pegmatite formation occurs in the presence of viscous, polymerized silicate magma and supercritical aqueous fluid (e.g. Dharmapriya et al., 2021). The pegmatite formation process is a continuous physico-chemical transitional process, progressing from magmatic to hydrothermal temperatures and pressures, making it challenging to precisely determine which hypothesis is involved.

Using experimental data, stable isotopic data, fluid inclusion analysis, and thermal modelling, researchers have attempted to speculate on the pressure-temperature (P-T) evolution of pegmatites (e.g., Jahns and Burnham, 1969; Babu, 1969; Taylor et al., 1979; Kosukhin et al., 1984; Simmons et al., 1987; Bakumenko and Konovalenko, 1988; Chakoumakos and Lumpkin, 1990; Sirbescu and Nabelek, 2003a, b; London et al., 2012a). Results indicate that the crystallization temperature conditions range from 700 to 300 °C at 2–5 kbar, with a rapid crystallization process compared to typical plutonic rocks.

Pegmatites are classified based on depth of emplacement, P-T conditions, and geochemical signatures (Ginsburg et al., 1979; Černý, 1991a; Zagorsky et al., 1999; Wise, 1999; Pezzotta, 2001; Černý and Erict, 2005; Martin and De Vito, 2005; Fuchsloch et al., 2018; Beskin and Marin, 2018). Geochemical classification, mainly based on rare earth element concentration, has improved over the last thirty years but remains somewhat complicated. Overlapping geochemical signatures among different pegmatites can occur due to the complexity of the parent magma (Martin and De Vito, 2005). Additionally, the geochemical signatures of original pegmatitic magma may be overprinted by contamination from surrounding country rocks. The classification schemes also do not encompass the most dominant ceramic/barren pegmatites, constituting over 99% of all known pegmatite bodies worldwide (London, 2008).

Studies reveal that granitic pegmatites predominantly form in tectonically active settings, particularly during supercontinent cycles and associated collisional or extensional events. The observed correlation between pegmatite ages and supercontinent assembly underscores the influence of large-scale tectonic processes on pegmatite formation. Despite significant advances, there is a need for further research to elucidate the roles of specific tectonic processes, such as slab rollback and mantle plumes, in pegmatite genesis. Future investigations should integrate diverse geological data to refine models and enhance predictions of pegmatite occurrences and their economic potential worldwide.

CRediT authorship contribution statement

P.L. Dharmapriya: Writing – review & editing. **D.W.M. Disanayaka:** Writing – review & editing. **H.M.T.G.A. Pitawala:** Writing – review & editing, Conceptualization. **Sanjeewa P.K. Malaviarachchi:**

Writing – review & editing. **N.D. Subasinghe:** Writing – review & editing.

Declaration of competing interest

The authors declare the following financial interests/personal relationships which may be considered as potential competing interests: P. L. Dharmapriya reports financial support was provided by National Research Council, Sri Lanka. If there are other authors, they declare that they have no known competing financial interests or personal relationships that could have appeared to influence the work reported in this paper.

Acknowledgments

This paper is a product of the project “Petrogenesis, geochemistry and potential of economic mineralization of granitic pegmatite in Sri Lanka”, funded by the National Research Council, Sri Lanka (Grant No. NRC 19-092). We would like to express our sincere appreciation to Prof. Soumyajit Mukherjee, IIT Bombay, India, for handling and reviewing this manuscript. We also extend our deep gratitude to the anonymous reviewers for their valuable comments and suggestions, which significantly improved the earlier version of this manuscript.

Data availability

No data was used for the research described in the article.

References

Abdelfadil, K.M., Asimow, P.D., Azer, M.K., Gahlan, H.A., 2016. Genesis and petrology of Late Neoproterozoic pegmatites and aplites associated with the Taba metamorphic complex in southern Sinai, Egypt. Geol. Acta 14 (3), 0219-235.

Abduriyim, A., Kitawaki, H., Furuya, M., Schwarz, D., 2006. "Paraiba"-type copper-bearing tourmaline from Brazil, Nigeria, and Mozambique. Chemical fingerprinting by LA-ICP-MS. Gems and Gemology 42 (1), 4.

Altieri, A., Pezzotta, F., Skogby, H., Hålenius, U., Bosi, F., 2024. Tourmaline as a petrogenetic indicator highlighted in a multicoloured crystal from the gem deposit of Mavuco (Alto Ligoña pegmatite district, NE Mozambique). Mineral. Mag. 1–30.

Aranha, P.R.A., Adolf Heinrich, H.O.R.N., Joncew, H.C., 2018. Use of GPR in pegmatite mining: example of a sheetlike body from northern Minas Gerais, Brazil. Rom. J. Miner. Deposits 91 (1–2), 7–12.

Babu, V.R.R.M., 1969. Temperatures of formation of pegmatites of Nellore MicaBelt, Andhra Pradesh, India. Econ. Geol. 64, 66–71.

Badanina, E.V., Sitnikova, M.A., Gordienko, V.V., Melcher, F., Gäbler, H.E., Lodziak, J., Syritso, L.F., 2015. Mineral chemistry of columbite–tantalite from spodumene pegmatites of Kolmozero, Kola Peninsula (Russia). Ore Geol. Rev. 64, 720–735.

Bailey, S.W., 1980. Structures of layer silicates. In: Brindley, G.W., Brown, G. (Eds.), Crystal Structures of Clay Minerals and Their X-Ray Identification. Mineralogical Society, London, pp. 1–123.

Bakumenko, I.T., Konovalenko, S.I., 1988. Formation peculiarities of miarolitic pegmatites and their position among granitic pegmatites. In: Termobarogeokhimicheskie Issledovaniya Protsessov Mineraloobrazovaniya (Studies of Inclusions in Minerals with Applications to Mineralization Processes), Novosibirsk, pp. 123–135.

Ballouard, C., Elburg, M.A., Tappe, S., Reinke, C., Ueckermann, H., Doggart, S., 2020a. Magmatic-hydrothermal evolution of rare metal pegmatites from the Mesoproterozoic Orange River pegmatite belt (Namaqualand, South Africa). Ore Geol. Rev. 116, 103252.

Ballouard, C., Massuyeau, M., Elburg, M.A., Tappe, S., Viljoen, F., Brandenburg, J.T., 2020b. The magmatic and magmatic-hydrothermal evolution of felsic igneous rocks as seen through Nb-Ta geochemical fractionation, with implications for the origins of rare-metal mineralizations. Earth Sci. Rev. 203, 103115.

Bartels, A., Vetere, F., Holtz, F., Behrens, H., Linnen, R.L., 2011. Viscosity of flux-rich pegmatitic melts. Contrib. Mineral. Petrol. 162, 51–60.

Bassot, J.P., Morio, M., 1989. Morphologie et mise en place de la pegmatite kibarienne a Sn, Nb, Ta, Li de manonon (Zaïre). Chron. Rech. Min. 496, 41–56.

Bastin, E.S., 1910. Origin of the pegmatites of Maine. J. Geol. 18 (4), 297–320.

Bastin, E.S., 1911. Geology of the pegmatites and associated rocks of Maine: including feldspar, quartz, mica and gem deposits. Bulletin (Geological Survey (U.S.)) 445.

Berning, J., Cooke, R., Hiemstra, S.A., Hoffman, U., 1976. The Rössing uranium deposit, south west Africa. Econ. Geol. 71 (1), 351–368.

Beskin, S.M., Marin, Y.B., 2018. Classification of granitic pegmatites and pegmatite-bearing granitic systems. Geol. Ore Depos. 60 (7), 578–586.

Best, M.G., 2003. Igneous and Metamorphic Petrology, second ed. John Wiley & Sons, p. 729.

Beurlen, H., Thomas, R., Melgarejo, J.C., Da Silva, J.M.R., Rhede, D., Soares, D.R., Da Silva, M.R., 2013. Chrysoberyl-sillimanite association from the Roncadeira pegmatite, Borborema Province, Brazil: implications for gemstone exploration. J. Geosci. 58 (2), 79–90.

Beus, A., 1983. On the possible mechanism of formation of euhedral crystals in metasomatic processes. Bull. Miner. 106, 411–415.

Bhandari, S., Qin, K., Zhou, Q., Evans, N.J., Gyawali, B.R., He, C., Sun, Z., 2023. Magmatic-hydrothermal evolution of the aquamarine-bearing Yamrang Pegmatite, Eastern Nepal: insights from beryl, garnet, and tourmaline mineral chemistry. Ore Geol. Rev., 105713

Bjørlykke, H., 1937. The granite pegmatites of southern Norway. Am. Mineral. 22, 241–255.

Bourret, W., 1988. Uranium-bearing pegmatites of the Antsirabe-Kitsamby district, Madagascar. Ore Geol. Rev. 3 (1–3), 177–191.

Bradley, D.C., 2011. Secular trends in the geologic record and the supercontinent cycle. Earth Sci. Rev. v. 108, 16–33.

Bradley, D.C., 2019. Tectonic and paleoclimatic controls of lithium-cesium-tantalum (LCT) pegmatite genesis, exhumation, and preservation in the Appalachians. Can. Mineral. 57 (5), 715–717.

Bradley, D.C., McCauley, A.D., Stillings, L.L., 2017. Mineral-Deposit Model for Lithium-Cesium-Tantalum Pegmatites U.S. Geological Survey (Compiler), Reston, VA, Scientific Investigations Report; Geochronology Record 2010-5070O. Geological Survey of Western Australia, p. 58p.

Breaks, F.W., Selway, J.B., Tindle, A.C., 2005. Fertile peraluminous granites and related rare-element pegmatites, Superior Province of Ontario. In: Linnen, R.L., Sampson, I. M. (Eds.), Rare-Element Geochemistry and Mineral Deposits, Geol. Soc. Can. Short Course Notes, St. Catharines, vol. 17, pp. 87–125.

Brögger, W.C., 1890. Die mineralien der syenitpegmatitgänge der Sqdnorwegischenaugit und nephelinsyenite. Z. Kristallogr. Mineral. 16, 1–63.

Brotzen, O., 1959. Outline of mineralization in zoned granitic pegmatites: a qualitative and comparative study. Geol. Foren. Stockh. Forh. 81 (1), 1–98.

Brown, J.A., 2001. Mineralogy and Geochemistry of Alkali Feldspars from the Tanco Pegmatite, Southeastern Manitoba. Univ. Manitoba, Winnipeg, Manitoba. M.Sc. thesis.

Brown, J.A., Martins, T., ČernÝ, P., 2017. The Tanco pegmatite at Bernic Lake, Manitoba. XVII. Mineralogy and geochemistry of alkali feldspars. Can. Mineral. 55 (3), 483–500.

Bushev, A.G., Koplus, A.V., 1980. Rare-earth pegmatites of the granulite facies of metamorphism. Int. Geol. Rev. 22, 221–232.

Camacho, A., Baadsgaard, H., Davis, D.W., Černý, P., 2012. Radiogenic isotope systematics of the Tanco and Silverleaf granitic pegmatites, Winnipeg River pegmatite district, Manitoba. Can. Mineral. 50 (6), 1775–1792.

Cameron, E.N., Jahns, R.H., McNair, A.H., Page, L.R., 1949. Internal structure of granitic pegmatites. Econ. Geol. Monogr. 2, 115.

Cardoso-Fernandes, J., Santos, D., Rodrigues de Almeida, C., Lima, A., Teodoro, A.C., GREENPEG Project Team, 2023. Spectral library of European pegmatites, pegmatite minerals and pegmatite host-rocks–the GREENPEG project database. Earth Syst. Sci. Data 15 (7), 3111–3129.

Černý, P., 1972. The Tanco pegmatite at Bernic Lake, Manitoba: VIII, secondary minerals from the spodumene-rich zones. Can. Mineral. 11, 714–726.

Černý, P., 1991a. Rare-element granitic pegmatites. Part I: anatomy and internal evolution of pegmatitic deposits. Geosci. Can. 18 (2), 49–67.

Černý, P., 1991b. Rare-element granitic pegmatites. Part II: regional to global environments and petrogenesis. Geosci. Can. 18 (2), 67–81.

Černý, P., Ercit, T.S., 1985. Some recent advances in the mineralogy and geochemistry of Nb and Ta in rare-element granitic pegmatites. Bull. Mineral. 108 (3), 499–532.

Černý, P., Ercit, T.S., 2005. The classification of granitic pegmatites revisited. Can. Mineral. 43, 2005–2026.

Černý, P., Siivola, J., 1980. The Tanco pegmatite at Bernic Lake. Manitoba. XII. Hafnian zircon. Canadian Mineralogists 18, 313–321.

Černý, P., Anderson, A.J., Tomascak, P.B., Chapman, R., 2003. Geochemical and morphological features of beryl from the Bikita granitic pegmatite, Zimbabwe. Can. Mineral. 41 (4), 1003–1011.

Černý, P., Masau, M., Goad, B.E., Ferreira, K., 2005. The Greer Lake leucogranite, Manitoba, and the origin of lepidolite-subtype granitic pegmatites. Lithos 80 (1–4), 305–321.

Černý, P., London, D., Novák, M., 2012. Granitic pegmatites as reflections of their sources. Elements 8 (4), 289–294.

Chadwick, R.A., 1958. Mechanisms of pegmatite emplacement. Geol. Soc. Am. Bull. 69 (7), 803–836.

Chagondah, G.S., Kramers, J.D., Hofmann, A., Rollinson, H., 2024. Neoarchaean and Palaeoproterozoic tectono-metamorphic events along the southern margin of the Zimbabwe craton: insights from muscovite 40Ar/39Ar geochronology from rare-metal pegmatites, Zimbabwe. J. Afr. Earth Sci. 217, 105333.

Chakoumakos, B.C., Lumpkin, G.R., 1990. Pressure-temperature constraints on the crystallization of the Harding pegmatite. Taos County, New Mexico. Canadian Mineralologist 28, 287–298.

Chakraborty, T., Büttner, S.H., Costin, G., Kankuzi, C.F., 2024. The petrogenesis of highly fractionated gem-bearing pegmatites of Malawi: evidence from mica and tourmaline chemistry and finite step trace element modelling. Miner. Deposita 59 (4), 837–857.

Chappell, B.W., White, A.J.R., 1992. I-And S-type granites in the lachlan Fold Belt. Earth Environ. Sci. Transact. Royal Soci. Edinburgh 83 (1–2), 1–26.

Chiarenzelli, J., Lupulescu, M., Robinson, G., Bailey, D., Singer, J., 2019. Age and origin of silicocarbonate pegmatites of the Adirondack region. Minerals 9 (9), 508.

Christiansen, E.H., Haapala, I., Hart, G.L., 2007. Are Cenozoic topaz rhyolites the erupted equivalents of Proterozoic rapakivi granites? Examples from the western United States and Finland. Lithos 97 (1–2), 219–246. Lv.

Clifford, J.H., 2012. Connoisseur's Choice: Rose (Pink) Quartz Lavra da Pitorra, Laranjeiras, Galiléia Minas Gerais, Brazil. Rocks Miner. 87 (6), 530–539.

Condie, K.C., Belousova, E., Griffin, K.L., Sircombe, K.N., 2009. Granitoid events in space and time: constraints from igneous and detrital zircon age spectra. Gondwana Res. 15, 228–242.

Cornejo, C., Bartorelli, A., 2010. Minerals and Precious Stones of Brazil. Solaris Cultural Publications, São Paulo, Brazil, p. 704.

Cronwright, M., 2014. A review of the rare-element pegmatites of the Alto Ligonha Pegmatite Province, northern Mozambique. In: Abstract Volume of the 21st General Meeting of the International Mineralogical Association, vol. 1.

De Mello, F.M., Bilal, E., 2012. Ages constraints in pegmatite province related to charnockitic host rocks in Minas Gerais, Brazil. Rom. J. Miner. Deposits 85 (1), 94–98.

Dewaele, S., Hulsbosch, N., Cryns, Y., Boyce, A., Burgess, R., Muchez, P., 2016. Geological setting and timing of the world-class Sn, Nb–Ta and Li mineralization of manono-Kitotolo (Katanga, Democratic Republic of Congo). Ore Geol. Rev. 72, 373–390.

Dharmapriya, P.L., Disanayaka, D.W.M., Martin, R.F., Pitawala, H.M.T.G.A., Malaviarachchi, S.P., 2021. Granitic pegmatites in Sri Lanka: a concise review leading to insights and predictions. Ore Energy Resour. Geol. 6, 100011.

Dill, H.G., 2015. Pegmatites and aplites: their genetic and applied ore geology. Ore Geol. Rev. 69, 417–561.

Dill, H.G., 2016. The CMS classification scheme (Chemical composition – mineral assemblage – structural geology) – linking geology to mineralogy of pegmatitic and aplitic rocks. Neues Jahrbuch fur Mineralogie Abhandlungen 193/3, 231–263.

Dingwell, D.B., Hess, K.U., Knoche, R., 1996. Granite and granitic pegmatite melts: volumes and viscosities. Earth Environ. Sci. Transact. Royal Soci. Edinburgh 87 (1–2), 65–72.

Dittrich, T., Seifert, T., Schulz, B., Hagemann, S., Gerdes, A., Pfänder, J., Dittrich, T., Seifert, T., Schulz, B., Hagemann, S., Gerdes, A., 2019. Introduction to Archean rare-metal pegmatites. In: Archean Rare-Metal Pegmatites in Zimbabwe and Western Australia: Geology and Metallogeny of Pollucite Mineralisations, pp. 1–21.

Dixon, J.B., 1989. Kaolin and serpentine group minerals. Mineral. Soil Environ. 1, 467–525.

Dostal, J., Kontak, D.J., Gerel, O., Shellnutt, J.G., Fayek, M., 2015. Cretaceous ongonites (topaz-bearing albite-rich microleucogranites) from Ongon Khairkhan, Central Mongolia: products of extreme magmatic fractionation and pervasive metasomatic fluid: rock interaction. Lithos 236, 173–189.

Dwight, B., Andrew, M., 2013. A Preliminary Deposit Model for Lithium-Cesium-Tantalum (LCT) Pegmatites (Ver. 1.1, December 2016), vols. 2013–1008. U.S. Geological Survey Open-File Report, p. 7.

Eagle, R.M., Birch, W.D., McKnight, S., 2015. Phosphate minerals in granitic pegmatites from the Mount Wills district, north-eastern Victoria. Proc. Roy. Soc. Vic. 127 (2), 55–68.

Eby, G.N., 1990. The A-type granitoids: a review of their occurrence and chemical characteristics and speculations on their petrogenesis. Lithos 26 (1–2), 115–134.

Eeckhout, S.G., Castañeda, C., Ferreira, A.C.M., Sabioni, A.C., De Grave, E., Vasconcelos, D.C., 2002. Spectroscopic studies of spessartine from Brazilian pegmatites. Am. Mineral. 87 (10), 1297–1306.

Ekosse, G.I.E., 2010. Kaolin deposits and occurrences in Africa: geology, mineralogy and utilization. Appl. Clay Sci. 50 (2), 212–236.

Ercit, T.S., 2004. REE-enriched granitic pegmatites. Rare element geochemistry and ore deposits. In: Linnen, R.L., Samson, I.M. (Eds.), Geological Association of Canada. Short Course Notes, vol. 17, pp. 257–296.

Falster, A.U., Simmons, Wm.B., Webber, K.L., 1997. The Origin of Evolved LCT-type Granitic Pegmatites in the Hoskin Lake Granite-Pegmatite Field, Florence Co. IAVCEI General Assembly, Jan. 1997, Puerto Vallarta, Mexico, Programme, Wisconsin, p. 118.

Falster, A.U., Simmons, W.B., Webber, K.L., 2001. Unorthodox compositional trends in columbite-group minerals from the Animikie red Ace pegmatite, Wisconsin, USA. J. Czech Geol. Soc. 46 (1–2), 69–79.

Falster, A.U., Simmons, Wm.B., Webber, K.L., 2005. Origin of the pegmatites in the Hoskin lake pegmatite field, Florence Co., Wisconsin. Crystallization processes in granitic pegmatites, Intl Meeting, Elba Island, Italy. MSA web site. http://www.minsocam.org/MSA/Special/Pig/PIG_articles/Elba%20Abstracts%207%20Falster.pdf.

Federico, M., Andreozzi, G.B., Lucchesi, S., Graziani, G., Cesar Mendes, J., 1998. Compositional variation of tourmaline in the granitic pegmatite dykes of the Cruzeiro mine, Minas Gerais, Brazil. Can. Mineral. 36 (2), 415–431.

Fei, G., Li, B., Yang, J., Chen, X., Luo, W., Li, Y., Tang, W., Gu, C., Zhong, W., Yang, G., 2018. Geology, fluid inclusion characteristics and H–O–C isotopes of large L ijiagou pegmatite spodumene deposit in S ongpan–G arze Fold Belt, E astern T ibet: I mplications for ore genesis. Resour. Geol. 68 (1), 37–50.

Fei, G., Menuge, J.F., Chen, C., Yang, Y., Deng, Y., Li, Y., Zheng, L., 2021. Evolution of pegmatite ore-forming fluid: the Lijiagou spodumene pegmatites in the Songpan-Garze Fold Belt, southwestern Sichuan province, China. Ore Geol. Rev. 139, 104441.

Feng, Y., Cen, J., Liang, T., Wang, M., Tan, X., Hao, Y., Yan, S., 2023. Lithium, Phosphorus, and rare earth elements in magmatic garnets from granitic Pegmatites: Coupled substitution and petrogenetic implications. Ore Geol. Rev. 153, 105284.

Fenn, P.M., 1977. The nucleation and growth of alkali feldspars from hydrous melts. Can. Mineral. 15, 135–161.

Fenn, P.M., 1986. On the origin of graphic granite. Am. Mineral. 71, 325–330.

Ferrero, R.C., Kolak, J.J., Bills, D.J., Bowen, Z.H., Cordier, D.J., Gallegos, T.J., Schmidt, J.M., 2013. US Geological Survey Energy and Minerals Science Strategy - A Resource Lifecycle Approach. US Department of the Interior, US Geological Survey, p. 52.

Fersman, A., 1930. A Geochemical Genetic Classification of Pegmatites. Monograph AkademiiaNauk SSSR, Moscow (in Russian).

Fersman, A., 1967. A geochemical genetic classification of pegmatites. In: Mather, K.F. (Ed.), A Source Book in Geology (1900–1950). Harvard University Press, Cambridge, Massachusetts, pp. 180–192.

Foord, E.E., 1982. Amazonite-bearing pegmatites of the Lake George intrusive center. In: Geological Association of Canada. – Mineralogical Association of Canada Annual Meeting, Field Trip Guidebook, vol. 12, pp. 51–56.

Fredriksson, J.R., 2017. Fluid Inclusion and Trace-Element Analysis of the Rare-Element Pegmatite Bodies Altim and Tamanduá from the Borborema Province. Brazil.

Frindt, S., Poutiainen, M., 2002. PT path fluid evolution in the Gross Spitzkoppe granite stock, Namibia. Bull. Geol. Soc. Finland 74 (1/2), 103–114.

Fuchsloch, W.C., Nex, P.A., Kinnaird, J.A., 2018. Classification, mineralogical and geochemical variations in pegmatites of the Cape Cross-Uis pegmatite belt, Namibia. Lithos 296, 79–95.

Gadas, P., Novák, M., Staněk, J., Filip, J., Vašinová Galiová, M., 2012. Compositional evolution of zoned tourmaline crystals from pockets in common pegmatites of the moldanubian zone, Czech Republic. Can. Mineral. 50 (4), 895–912, 2012.

Galeschuk, C., Vanstone, P., 2007. Exploration techniques for rare-element pegmatite in the Bird River greenstone belt, southeastern Manitoba. Proc. Exploration 7, 823–839. September.

Gao, J., Wei, G.Y., Li, G., Yin, Y.S., Zhang, R., Ling, H.F., Xu, Z., 2024. Geochemical constraints on the origin of the rare metal mineralization in granite-pegmatite, evidence from three-kilometer scientific drilling core in the Jiajika Li deposit, eastern Tibetan Plateau. Ore Geol. Rev. 165, 105852.

Georgieva, S., Vassileva, R., Milenkov, G., Stefanova, E., 2022. Major and trace element signature of epidote-group minerals in altered pegmatites from the Petrovitsa Pb–Zn deposit of the Madan ore region, Central Rhodopes, Bulgaria: evidence of allanite/epidote transformation. Geol. Carpathica 73 (4), 365–380.

Gillespie, M., Styles, M., 1999. BGS Rock Classification Scheme, Volume 1. Classification of Igneous rocks.British Geological Survey Research Report, second ed. RR 99–06.

Ginsburg, A.I., 1984. The geological condition of the location and the formation of granitic pegmatites. In: Proceedings of the 27th International Geological Congress, Non-metallic Mineral Ores, vol. 15, pp. 245–260.

Ginsburg, A.I., Rodionov, G.G., 1960. On the depth of formation of granitic pegmatites. Geol. Rudn. Mestorozhdeniy 1, 45–54 (in Russian).

Ginsburg, A.I., Timofeyev, L.N., Feldman, L.G., 1979. Principles of Geology of the Granitic Pegmatites. Nedra, Moscow, p. 296 (in Russian).

Glover, A.S., Rogers, W.Z., Barton, J.E., 2012. Granitic pegmatites: storehouses of industrial minerals. Elements 8 (4), 269–273.

Gogodo, A.S., 2021. *A Review of the Geology, Mineralisation, and Structural Controls on the Emplacement of the Bikita LCT Pegmatites, Masvingo Greenstone Belt, Zimbabwe Craton* (Doctoral Dissertation. Faculty of Science, University of the Witwatersrand, Johannesburg.

Gomes, C.L., Neiva, A.M., 2022. Tourmalines in the Namacotche Li-Cs-Ta Granitic Pegmatite Group, Mozambique: Crystal Chemistry and Origin.

Gomes, C.L., Dias, P.A., Guimarães, F., Castro, P., 2009. Microlites and associated oxide minerals from Naipa pegmatites, Alto Ligonha, Zambezia, Mozambique. EstudosGeológicos 19 (2), 167–171, 2009.

Goodenough, K.M., Shaw, R.A., Smith, M., Estrade, G., Marqu, E., Bernard, C., Nex, P., 2019. Economic mineralization in pegmatites: comparing and contrasting NYF and LCT examples. Can. Mineral. 57 (5), 753–755.

Gorlov, N.V., 1975. Structural principles of exploration for pegmatite deposits in northwestern White Sea region. In: Muscovite Pegmatites of the USSR. Nauka, Leningrad, USSR, pp. 146–153 in Russ.

Groat, L.A., Giuliani, G., Marshall, D.D., Turner, D., 2007. Emerald. In: Groat, L.A. (Ed.), Geology of Gem Deposits. Mineralogical Association Canada Short Course, vol. 37, pp. 79–109.

Harben, P.W., 2002. The Industrial Mineral Handybook—A Guide to Markets, Specifications and Prices, fourth ed. Industrial Mineral Information.Worcester Park, United Kingdom, p. 412.

Herath, J.W., 1985. Economic geology of Sri Lanka. Natural Resources Series: No. 1. NARESA:Colombo Sri Lanka 207.

Hickman, A.H., 1983. Geology of the Pilbara block and its environs. Geological survey of western Australia. Bulletin 127, 268.

Holtz, F., Johannes, W., Tamic, N., Behrens, H., 2001. Maximum and minimum water contents of granitic melts generated in the crust: a reevaluation and implications. Lithos 56 (1), 1–14.

Horton Jr., J.W., Sutter, J.F., Stern, T.W., Milton, D.J., 1987. Alleghanian deformation, metamorphism, and granite emplacement in the central Piedmont of the southern Appalachians. Am. J. Sci. 287, 635–660.

Hulsbosch, N., Hertogen, J., Dewaele, S., André, L., Muchez, P., 2014. Alkali metal and rare earth element evolution of rock-forming minerals from the Gatumba area pegmatites (Rwanda): Quantitative assessment of crystal-melt fractionation in the regional zonation of pegmatite groups. Geochem. Cosmochim. Acta 132, 349–374.

Hunt, T.S., 1871. Notes on granitic rocks. Am. J. Sci. (3), 182–191.

Hussain, A., Shah, M.T., Arif, M., Agheem, M.H., Mughal, M.S., Ullah, S., Hussain, S.A., Sadiq, I., 2021. Chemical composition of gemstones and characterization of their host pegmatites and country rocks from Chumar Bakhoor, Gilgit-Baltistan, Pakistan: implications for the source of gem-forming fluids. Arabian J. Geosci. 14, 1–15.

Jacobson, M.I., 2021. Where of mineral Names: Wodginite, Wodgina, Abydos station, western Australia. Rocks Miner. 96 (3), 264–269.

Jahns, R.H., 1953. The genesis of pegmatites: I. Occurrence and origin of giant crystals. Am. Mineral.: J. Earth Planetary Mater. 38 (7–8), 563–598.

Jahns, R.H., 1955. In: Bateman, A.M. (Ed.), The Study of Pegmatites; B Economic Geology, Fiftiethhniversary Volume, pp. 1025–1130.

Jahns, R.H., 1982. Internal evolution of pegmatite bodies. In: Černý, P. (Ed.), Granitic Pegmatites in Science and Industry, Mineral. Association Cananda. Short Course Handbook, vol. 8, pp. 293–327.

Jahns, R.H., Burnham, C.W., 1969. Experimental studies of pegmatite genesis; l, A model for the derivation and crystallization of granitic pegmatites. Econ. Geol. 64 (8), 843–864.

Jahns, R.H., Tuttle, O.F., 1963. Layered pegmatite-aplite intrusives. Min. Soc. Amer. Special Paper 1, 78–92.

Jahns, R.H., Griffitts, W.R., Heinrich, E.W., 1952. Mica deposits of the southeastern Piedmont. 1. General features. U.S. Geol. Surv., Prof. Pap. 248–A, 1–99.

Jain, A.K., Banerjee, D.M., Kale, V.S., Jain, A.K., Banerjee, D.M., Kale, V.S., 2020. Indian cratons. Tectonics of the Indian Subcontinent 17–122.

Jiankang, L., Denghong, W., Yuchuan, C., 2013. The ore-forming mechanism of the Jiajika pegmatite-type rare metal deposit in western Sichuan province: evidence from isotope dating. Acta GeologicaSinica-English Edition 87 (1), 91–101.

Kaeter, D., Barros, R., Menuge, J.F., Chew, D.M., 2018. The magmatic–hydrothermal transition in rare-element pegmatites from southeast Ireland: LA-ICP-MS chemical mapping of muscovite and columbite–tantalite. Geochem. Cosmochim. Acta 240, 98–130.

Kamenetsky, V.S., van Achterbergh, E., Ryan, C.G., Naumov, V.B., Mernagh, T.P., Davidson, P., 2002. Extreme chemical heterogeneity of granite-derived hydrothermal fluids: an example from inclusions in a single crystal of miarolitic quartz. Geology 30 (5), 459–462.

Keller, P.C., 1990. Gemstones formed in pegmatites: gem pegmatites of Minas Gerais, Brazil. In: Gemstones and Their Origins. Springer, Boston, MA, pp. 57–69.

Keppler, H., 1993. Influence of fluorine on the enrichment of high field strength trace elements in granitic rocks. Contrib. Mineral. Petrol. 114, 479–488.

Kesler, T.L., 1961. Exploration of the kings mountain pegmatites. Min. Eng. 13 (9), 1062–1068.

Kesler, S.E., Gruber, P.W., Medina, P.A., Keoleian, G.A., Everson, M.P., Wallington, T.J., 2012. Global lithium resources: relative importance of pegmatite, brine and other deposits. Ore Geol. Rev. 48, 55–69.

King, P.L., White, A.J.R., Chappell, B.W., Allen, C.M., 1997. Characterization and origin of aluminous A-type granites from the Lachlan Fold Belt, southeastern Australia. J. petrol. 38 (3), 371–391.

Kinnaird, J.A., 1985. Hydrothermal alteration and mineralization of the alkaline anorogenic ring complexes of Nigeria. J. Afr. Earth Sci. 3 (1–2), 229–251, 1983.

Klausen, M.B., 2020. Conditioned duality between supercontinental ‘assembly’ and ‘breakup’ LIPs. Geosci. Front. 11 (5), 1635–1649.

Klementová, M., Rieder, M., 2004. Exsolution in niobian rutile from the pegmatite deposit at Greenbushes, Australia. Can. Mineral. 42, 1859–1870.

Knoll, T., Huet, B., Schuster, R., Mali, H., Ntaflos, T., Hauzenberger, C., 2023. Lithium pegmatite of anatectic origin–A case study from the Austroalpine Unit Pegmatite Province (Eastern European Alps): geological data and geochemical modeling. Ore Geol. Rev. 154, 105298.

Kontak, D.J., Dostal, J., Kyser, T.K., Archibald, D.A., 2002. A petrological, geochemical, isotopic and fluid-inclusion study of 370 ma pegmatite–aplite sheets, Peggys Cove, Nova Scotia, Canada. Can. Mineral. 40 (5), 1249–1286.

Kosukhin, O.N., Bakumenko, I.T., Chupin, V.P., 1984. Magmatic Stage of Formation of Granite Pegmatites. Nauka, Novosibirsk [in Russian].

Kovalenko, N.I., 1979. An Experimental Study of the Formation of Rare Metal Li-F Granites. Moscow Nauka (In Russian).

Kozłowski, A., 1978. Pneumatolytic and hydrothermal activity in the Karkonosze-Izera block. Acta Geol. Pol. 28 (2), 171–222.

Kozłowski, A., Sachanbiński, M., 2007. Karkonosze Intragranitic Pegmatites and Their Minerals, vol. 1. Granitoids in Poland, AM Monograph, pp. 155–178.

Landes, K.K., 1933. Origin and classification of pegmatites. Am. Mineral.: J. Earth Planetary Mater. 18 (2), 33–56.

Landes, K.K., 1937. Pegmatites and hydrothermal veins. Am. Mineral.: J. Earth Planetary Mater. 22 (5), 551–560.

Larsen, R.B., Polve, M., Juve, G., 2000. Granite pegmatite quartz from Evje-Iveland: trace element chemistry and implications for the formation of high-purity quartz. NorgesGeologiskeUndersokelse 436, 57–66.

Lazarenko, E.K., Pavlishin, V.I., Latysh, V.T., Sorokin, Y.G., 1973. Mineralogy and Genesis of Chamber Pegmatites of Volynia. Lvov State Univ. publishing house, Lvov, USSR (in Russion).

Lentz, D., 1992. Petrogenesis and geochemical composition of biotites in rare-element granitic pegmatites in the southwestern Grenville Province, Canada. Mineral. Petrol. 46 (3), 239–256.

Li, W.C., Chen, R.X., Zheng, Y.F., Li, Q., Hu, Z., 2013. Zirconological tracing of transition between aqueous fluid and hydrous melt in the crust: constraints from pegmatite vein and host gneiss in the Sulu orogen. Lithos 162, 157–174.

Li, J., Yan, Q., Li, P., Jacobson, M.I., 2023. Formation of granitic pegmatites during orogenies: indications from a case study of the pegmatites in China. Ore Geol. Rev. 156, 105391.

Linnen, R.L., 1998. The solubility of Nb-Ta-Zr-Hf-W in granitic melts with Li and Li+F: constraints for mineralization in rare metal granites and pegmatites. Econ. Geol. 93, 1013–1025.

Linnen, R.L., Cuney, M., 2005. Granite-related rare-element deposits and. experimental constraints on Ta-Nb-W-Sn-Zr-Hf mineralization. In: Linnen, R.L., Samson, I.M. (Eds.), Rare-Element Geochemistry and Mineral Deposits, vol. 17. Geological Association of Canada, Short Course Notes, pp. 45–68.

Linnen, R.L., Williams-Jones, A.E., 1994. The evolution of pegmatite-hosted Sn-W mineralization at Nong Sua, Thailand: evidence from fluid inclusions and stable isotopes. Geochem. Cosmochim. Acta 58 (2), 735–747.

Linnen, R.L., Van Lichtervelde, M., Černý, P., 2012. Granitic pegmatites as sources of strategic metals. Elements 8 (4), 275–280.

Liu, Y., Schmidt, C., Li, J., 2022a. Peralkalinity in peraluminous granitic pegmatites. I. Evidence from whewellite and hydrogen carbonate in fluid inclusions. Am. Mineral. 107, 233–238.

Liu, Y., Schmidt, C., Li, J., 2022b. Peralkalinity in peraluminous granitic pegmatites. II. Evidence from experiments on carbonate formation in spodumene-bearing assemblages. Am. Mineral. 107, 239–247.

London, D., 1984. Experimental phase equilibria in the system LiAlSiO$_4$ -SiO$_2$ -H$_2$O; A petrogenetic grid for lithium-rich pegmatites. Am. Mineral. 69, 995–1004.

London, D., 1986. The magmatic–hydrothermal transition in the Tanco rare-element pegmatite: evidence from fluid inclusions and phase equilibrium experiments. Am. Mineral. 71, 376–395.

London, D., 1992. The application of experimental petrology to the genesis and crystallization of granitic pegmatites. Canadian Mineralogists 30, 499–540.

London, D., 2005. Granitic pegmatites: an assessment of current concepts and directions for the future. Lithos 80 (1–4), 281–303.

London, D., 2008. Pegmatites. The Canadian Mineralogist, vol. 10. Special Publication, p. 347.

London, D., 2009. The origin of primary textures in granitic pegmatites. Can. Mineral. 47 (4), 697–724.

London, D., 2014. A petrologic assessment of internal zonation in granitic pegmatites. Lithos 184, 74–104, 61.

London, D., 2015. Reading pegmatites: Part 1—what beryl says. Rocks Miner. 90 (2), 138–153.

London, D., 2017. Reading pegmatites: part 3—what lithium minerals say. Rocks Miner. 92 (2), 144–157.

London, D., 2018. Ore-forming processes within granitic pegmatites. Ore Geol. Rev. 101 (94), 349–383.

London, D., 2022. A Rayleigh model of cesium fractionation in granite-pegmatite systems. Am. Mineral. 107 (1), 82–91.

London, D., 2024. The Tanco pegmatite at Bernic Lake Manitoba, Canada. Rocks Miner. 99 (1), 60–77.

London, D., Hervig, R.L., Morgan, G.B.V., 1988. Melt-vapor solubilities and elemental partitioning in peraluminous granite pegmatite systems: experimental results with Macusani glass at 200 MPa. Contrib. Mineral. Petrol. 99, 360–373.

London, D., Kontak, D.J., 2012. Granitic pegmatites: scientific wonders and economic bonanzas. Elements 8 (4), 257–261.

London, D., Morgan, G.B., 2012. The pegmatite puzzle. Elements 8 (4), 263–268.

London, D., Morgan VI, G.B., Acosta-Vigil, A., 2012a. Experimental simulations of anatexis and assimilation involving metapelite and granitic melt. Lithos 153, 292–307.

London, D., Morgan VI, G.B., Paul, K.A., Guttery, B.M., 2012b. Internal evolution of a miarolitic granitic pegmatite: the little three mine, ramona, California (USA). Can. Mineral. 50, 1025–1054.

Lv, Z.H., Zhang, H., Tang, Y., 2021. Anatexis origin of rare metal/earth pegmatites: evidences from the Permian pegmatites in the Chinese Altai. Lithos 380, 105865.

Lv, S.J., Dong, G.C., Zhao, Z.D., Luo, Z.B., Ketchaya, Y.B., Li, X.W., Yuan, W.M., 2024. The genesis of the Chakabeishan Li-(Be) pegmatite deposit in the northern Tibetan Plateau: evidence from fluid inclusion and lithium isotope. Ore Geol. Rev., 105965

MacLellan, H.E., Trembath, L.T., 1991. The role of quartz crystallization in the development and preservation of igneous texture in granitic rocks: experimental evidence at 1 kbar. Am. Mineral. 76, 1291–1305.

Maneta, V., Anderson, A.J., 2018. Monitoring the crystallization of water-saturated granitic melts in real time using the hydrothermal diamond anvil cell. Contrib. Mineral. Petrol. 173, 1–18.

Martin, R.F., 1988. The K-feldspar mineralogy of granites and rhyolites: a generalized case of pseudomorphism of the magmatic phase. Rend. Soc. Ital. Mineral. Petrol. 43 (2), 343–354.

Martin, R.F., De Vito, C., 2005. The patterns of enrichment in felsic pegmatites ultimately depend on tectonic setting. Can. Mineral. 43, 2027–2048.

Masoudi, F., Yardley, B.W.D., 2005. Magmatic and metamorphic fluids in pegmatite development: evidence from Borujerd Complex, Iran. J. Sci. Islam. Repub. Iran 16 (1), 43–53.

Mauthner, M., 2024. Southern California pegmatite gems. Rocks Miner. 99 (1), 10–15.

McBirney, A.R., Russell, W.J., 1987. Constitutional zone refining of magmatic intrusions. Struct. Dynam. Partial. Solidified Syst. 349–365.

McCauley, A., Bradley, D.C., 2014. The global age distribution of granitic pegmatites. Can. Mineral. 52 (2), 183–190.

McManus, C.E., McMillan, N.J., Harmon, R.S., Whitmore, R.C., De Lucia Jr., F.C., Miziolek, A.W., 2008. Use of laser induced breakdown spectroscopy in the determination of gem provenance: beryls. Appl. Opt. 47 (31), G72–G79.

Meintzer, R.E., 1987. The Mineralogy and Geochemistry of the Granitoid Rocks and Related Pegmatites of the Yellowknife Pegmatite Field, Northwest Territories. Ph.D. Thesis. Univ. of Manitoba, Winnipeg, Manitoba, Canada.

Melcher, F., Graupner, T., Henjes-Kunst, F., Oberthür, T., Sitnikova, M., Gäbler, E., Gerdes, A., Brätz, H., Davis, D., Dewaele, S., 2008. Analytical fingerprint of columbite–tantalite (coltan) mineralization in pegmatites: focus on Africa. Proceed. Ninth Intern. Congr. Appl. Mineral 8, 615–624.

Melcher, F., Graupner, T., Gäbler, H.E., Sitnikova, M., Henjes-Kunst, F., Oberthür, T., Dewaele, S., 2015. Tantalum–(niobium–tin) mineralisation in African pegmatites and rare metal granites: constraints from Ta–Nb oxide mineralogy, geochemistry and U–Pb geochronology. Ore Geol. Rev. 64, 667–719.

Menezes Filho, L.A.D., Chaves, M.L.D.S.C., Dias, C.H., Atencio, D., 2016. Recent mineral discoveries in the Coronel Murta, Taquaral, and Medina pegmatite fields, northeastern Minas Gerais, Brazil. REM-Int. Eng. J. 69 (3), 301–307.

Merritt, C.A., 1924. The Function of Gels in the Formation of Pegmatites and of Quartz and Carbonate Veins. University of Manitoba, Winnipeg, Manitoba, Canada. MSc thesis.

Morgan, G.B., London, D., 1987. Alteration of amphibolitic wallrocks around the Tanco rare-element pegmatite, Bernic Lake, Manitoba. Am. Mineral. 72 (11–12), 1097–1121.

Morgan, G.B., London, D., 1999. Crystallization of the little three layered pegmatite-aplite dike, Ramona district, California. Contrib. Mineral. Petrol. 136, 310–330.

Mukherjee, S., 2013. Channel flow extrusion model to constrain dynamic viscosity and Prandtl number of the Higher Himalayan Shear Zone. Int. J. Earth Sci. 102, 1811–1835.

Müller, A., Ihlen, P.M., Snook, B., Larsen, R.B., Flem, B., Bingen, B., Williamson, B.J., 2015. The chemistry of quartz in granitic pegmatites of southern Norway: petrogenetic and economic implications. Econ. Geol. 110 (7), 1737–1757.

Müller, A., Romer, R.L., Pedersen, R.B., 2017. The Sveconorwegian pegmatite province–thousands of pegmatites without parental granites. Can. Mineral. 55 (2), 283–315.

Müller, A., Spratt, J., Thomas, R., Williamson, B.J., Seltmann, R., 2018. Alkali-F-rich albite zones in evolved NYF pegmatites: the product of melt–melt immiscibility. Can. Mineral. 56 (4), 657–687.

Müller, A., Keyser, W., Simmons, W.B., Webber, K., Wise, M., Beurlen, H., Garate-Olave, I., Roda-Robles, E., Galliski, M.Á., 2021. Quartz chemistry of granitic pegmatites: implications for classification, genesis and exploration. Chem. Geol. 584, 120507.

Müller, A., Simmons, W., Beurlen, H., Thomas, R., Ihlen, P.M., Wise, M., Roda-Robles, E., Neiva, A.M., Zagorsky, V., 2022. A proposed new mineralogical classification system for granitic pegmatites–Part I: history and the need for a new classification. Can. Mineral. 60 (2), 203–227.

Munasinghe, T., Dissanayake, C., 1980. Are charnockites metamorphosed Archean volcanic rocks?—a case study from Sri Lanka. Precambr. Res. 12 (1–4), 459–470.

Murata, K.J., Dutra, C.V., Da Costa, M.T., Branco, J.J.R., 1959. Composition of monazites from pegmatites in eastern Minas Gerais, Brazil. Geochem. Cosmochim. Acta 16 (1–3), 1–14.

Murray, H.H., 1999. Applied clay mineralogy today and tomorrow. Clay Miner. 34 (1), 39–49.

Mustart, D.A., 1972. Phase Relations in the Peralkaline Portion of the System Na_2O-Al_2O_3-SiO_2-H_2o. PhD Thesis. Stanford Univ., Stanford, Calif.

Nabelek, P.I., Russ-Nabelek, C., Denison, J.R., 1992a. The generation and crystallization conditions of the Proterozoic Harney Peak leucogranite, Black Hills, South Dakota, USA: petrologic and geochemical constraints. Contrib. Mineral. Petrol. 110, 173–191.

Nabelek, P.I., Russ-Nabelek, C., Haeussler, G.T., 1992b. Stable isotope evidence for the petrogenesis and fluid evolution in the proterozoic Harney peak leucogranite, Black Hills, south Dakota. Geochem. Cosmochim. Acta 56, 403–417.

Ndikumana, J.D.D., Bolarinwa, A.T., Adeyemi, G.O., Olajide-Kayode, J., Nambaje, C., 2020. Geochemistry of feldspar and muscovite from pegmatite of the Gatumba area, Karagwe Ankole Belt: implications for Nb–Ta–Sn mineralisation and associated alterations. SN Appl. Sci. 2 (9), 1568.

Neiva, A.M., 2013. Micas, feldspars and columbite–tantalite minerals from the zoned granitic lepidolite-subtype pegmatite at Namivo, Alto Ligonha, Mozambique. Eur. J. Mineral 25 (6), 967–985.

Nete, M., 2009. Dissolution and analytical characterization of tantalite ore, niobium metal and other niobium compounds. In: Doctoral Dissertation, University of the Free State).

Niggli, P., 1920. Die leichtflüchtigenBestandteileim. Magma. Leipzig, pp. 1–272.

Oyarzábal, J., Galliski, M.Á., Perino, E., 2009. Geochemistry of K-feldspar and muscovite in rare-element pegmatites and granites from the Totoral Pegmatite Field, San Luis, Argentina. Resour. Geol. 59 (4), 315–329.

Palinkaš, S.S., Wegner, R., Čobić, A., Palinkaš, L.A., De Brito Barreto, S., Váczi, T., Bermanec, V., 2014. The role of magmatic and hydrothermal processes in the evolution of Be-bearing pegmatites: evidence from beryl and its breakdown products. Am. Mineral. 99 (2–3), 424–432.

Partington, G.A., McNaughton, N.J., Williams, I.S., 1995. A review of the geology, mineralization, and geochronology of the Greenbushes pegmatite, Western Australia. Econ. Geol. 90 (3), 616–635.

Pattison, D.R.M., DeBuhr, C.L., 2015. Petrology of metapelites in the bugaboo aureole, British Columbia, Canada. J. Metamorph. Geol. 33 (5), 437–462.

Peretyazhko, I.S., 2010. Genesis of mineralized cavities (miaroles) in granitic pegmatites and granites. Petrology 18, 183–208.

Pezzotta, F., 2001. Madagascar's rich pegmatite districts: a general classification. In: "Madagascar, extraLapis English No. 1", Lapis Intl. LLC, pp. 34–35. East Hampton, CT.

Pezzotta, F., 2005. First attempt to the petrogenesis and the classification of granitic pegmatites of the Itremo Region (central Madagascar). In: International Meeting on Crystallization Processes in Granitic Pegmatites, Elba.

Pezzotta, F., Laurs, B.M., 2011. Tourmaline: the kaleidoscopic gemstone. Elements 7 (5), 333–338.

Phelps-Barber, Z., Trench, A., Groves, D.I., 2022. Recent pegmatite-hosted spodumene discoveries in Western Australia: insights for lithium exploration in Australia and globally. Appl. Earth Sci. 131 (2), 100–113.

Prasad, M.S., Reid, K.J., Murray, H.H., 1991. Kaolin: processing, properties and applications. Appl. Clay Sci. 6 (2), 87–119.

Proctor, K., 1985. Gem pegmatites of Minas Gerais, Brazil: the tourmalines of the Araçuai districts. Gems Gemol. 2 (1), 3–19.

Ramberg, H., 1952. The Origin of Metamorphic and Metasomatic Rocks: a Treatise on Recrystallization and Replacement in the Earth's Crust. University of Chicago Press.

Rao, C., Wang, R., Yang, Y., Hatert, F., Xia, Q., Yue, X., Wang, W., 2017. Insights into post-magmatic metasomatism and Li circulation in granitic systems from phosphate minerals of the Nanping No. 31 pegmatite (SE China). Ore Geol. Rev. 91, 864–876.

Reitan, P.H., 1965. Pegmatite veins and the surrounding rocks. V. Secondary recrystallization of aplite to form pegmatite. Norsk. Geol. Tidsskr. 45, 31–40.

Richter, L., Dittrich, T., Seifert, T., Schulz, B., 2014. LCT pegmatites from the Wodgina pegmatite district, Western Australia. In: EGU General Assembly Conference Abstracts, p. 6658. May.

Rino, S., Kon, Y., Sato, W., Maruyama, S., Santosh, M., Zhao, D., 2008. The Grenvillian and Pan-African orogens: world's largest orogenies through geologic time, and their implications on the origin of superplume. Gondwana Res. 14 (1–2), 51–72.

Robie, R.A., Hemingway, B.S., 1984. Entropies of kyanite, andalusite, and sillimanite: additional constraints on the pressure and temperature of the Al_2SiO_5 triple point. Am. Mineral. 69 (3–4), 298–306.

Roda, E., Vieira, R., Lima, A., Pesquera, A., Noronha, F., Fontan, F., 2007. The Fregeneda–Almendra pegmatitic field (Spain & Portugal): mineral assemblages and regional zonation. In: Granitic Pegmatites: the State of the Art – International Symposium. 06th – 12th May 2007, Porto, Portugal.

Roda-Robles, E., Vieira, R., Pesquera, A., Lima, A., 2010. Chemical variations and significance of phosphates from the Fregeneda-Almendra pegmatite field, Central Iberian Zone (Spain and Portugal). Mineral. Petrol. 100, 23–34.

Roda-Robles, E., Vieira, R., Lima, A., Errandonea-Martin, J., Pesquera, A., Cardoso-Fernandes, J., Garate-Olave, I., 2023. Li-rich pegmatites and related peraluminous granites of the Fregeneda-Almendra field (Spain-Portugal): a case study of magmatic signature for Li enrichment. Lithos 452, 107195.

Roedder, E., 1981. Natural occurrence and significance of fluids indicating high pressure and temperature. Phys. Chem. Earth 13, 9–39.

Roedder, E., 1992. Fluid inclusion evidence for immiscibility in magmatic differentiation. Geochem. Cosmochim. Acta 56 (1), 5–20.

Rosing-Schow, N., Romer, R.L., Müller, A., Corfu, F., Škoda, R., Friis, H., 2023. Geochronological constraints for a two-stage history of the Sveconorwegian rare-element pegmatite province formation. Precambr. Res. 384, 106944.

Sánchez-Muñoz, L., Müller, A., Andrés, S.L., Martin, R.F., Modreski, P.J., de Moura, O.J., 2017. The P–Fe diagram for K-feldspars: a preliminary approach in the discrimination of pegmatites. Lithos 272, 116–127.

Schaller, W.T., 1925. The genesis of lithium pegmatitns. Am. J. Sci. 10, 269–279.

Schneiderhöhn, 1961. Ore Deposits of the World. Volume II. Pegmatites. Gustav Fischer Verlag, Stuttgart (classification on page 628, in German).

Scholz, R., Chaves, M.L.S.C., Krambrock, K., 2011. Mineralogy of the lithium bearing pegmatites from the Conselheiro Pena pegmatite district (Minas Gerais, Brazil). AsociaciónGeológica Argentina D 14, 193–195.

Schwarz, D., Giuliani, G., Grundmann, G., Glas, M., 2002. The origin of emerald. Emeralds of the World. Extra Lapis English 2, 10–15.

Selway, J.B., Breaks, F.W., Tindle, A.G., 2005. A review of rare-element (Li-Cs-Ta) pegmatite exploration techniques for the Superior Province, Canada, and large worldwide tantalum deposits. Explor. Min. Geol. 14 (1–4), 1–30.

Shaw, R.A., Goodenough, K.M., Roberts, N.M.W., Horstwood, M.S.A., Chenery, S.R., Gunn, A.G., 2016. Petrogenesis of rare-metal pegmatites in high-grade metamorphic terranes: a case study from the Lewisian Gneiss Complex of north-west Scotland. Precambr. Res. 281, 338–362.

Shearer, C.K., Papike, J.J., Simon, S.B., Laul, J.C., 1986. Pegmatite-wallrock interactions, Black Hills, South Dakota; interaction between pegmatite-derived fluids and quartz-mica schist wallrock. Am. Mineral. 71 (3–4), 518–539.

Shelley, D., 1993. Igneous and Metamorphic Rocks under the Mcroscope: Classification, Textures, Microstructures and Mineral Preferred Orientations. Chapman & Hall, New York, p. 445p.

Shigley, E.L., Anthony, R., Kampf, A.R., 1984. Gem-bearing pegmtites : a review. Gems and Geommology 20, 64–77.

Shigley, J.E., Laurs, B.M., Janse, A.J.A., Elen, S., Dirlam, D.M., 2010. Gem localities of the 2000s. Gems Gemol. 46 (3).

Shmakin, B.M., 1976. Muscovite and Rare Metal – Muscovite Pegmatites. Nauka, Novosibirsk. USSR (in Russ.).

Simmons, W.B.S., 2005. A look at pegmatite classifications. In: Crystallization Processes in Granitic Pegmatites-International Meeting Abstracts-23rd-29th May.

Simmons, W.B.S., 2007. Gem-bearing pegmatites. In: Groat, L.A. (Ed.), Geology of Gem Deposits. Mineralogical Association Canada Short Course, vol. 37, pp. 169–206.

Simmons, W.B.S., Webber, K.L., 2008. Pegmatite genesis: state of the art. Eur. J. Mineral 20 (4), 421–438.

Simmons, W.B., Lee, M.T., Brewster, R.H., 1987. Geochemistry and evolution of the South Platte granite-pegmatite system, Jefferson county, Colorado. Geochem. Cosmochim. Acta 51 (3), 455–471.

Simmons, Wm.B., Foord, E.E., Falster, A.U., King, V.T., 1995. Evidence for an anatectic origin of granitic pegmatites, western Maine, USA. In: Geological Society of America, Annual Meeting., New Orleans, LA, Abstract Proceeding, vol. 27, p. A411.

Simmons, Wm.B., Foord, E.E., Falster, A.U., 1996. Anatectic origin of granitic pegmatites, western Maine, USA. In: GAC-MAC Geological Society of America, Annual Meeting., New Orleans, LA, Abstract Proceeding., A87.

Simmons, W.B., Pezzotta, F., Shigley, J.E., Beurlen, H., 2012. Granitic pegmatites as sources of colored gemstones. Elements 8 (4), 281–287.

Simmons, W., Falster, A., Webber, K., Roda-Robles, E., Boudreaux, A.P., Grassi, L.R., Freeman, G., 2016. Bulk composition of Mt. Mica pegmatite, Maine, USA:

implications for the origin of an LCT type pegmatite by anatexis. Can. Mineral. 54 (4), 1053–1070.

Simmons, W.B., Webber, K.L., Falster, A.U., 2018. Post-orogenic, pre-rifting anatectic origin of the Oxford County, Maine pegmatite field. In: International Mineralogical Association 2018, vol. 288. *abstract volume*.

Simmons, W.B., Webber, K.L., Falster, A.U., 2024. Pegmatites. Rocks & Minerals 99 (1), 18–32.

Simmons, William B., Webber, Karen L., Falster, Alexander U., 2024. Pegmatites, rocks &amp. Minerals 99 (1), 18–32.

Sinclair, W.D., 1995. Granitic pegmatites. Geology of Canadian Mineral Deposit Types. O.R. Eckstrand, W.D. Sinclair, R.I. Thorpe.

Sirbescu, M.-L., Nabelek, P., 2003a. Crustal melts below 400 ∘C. Geology 31, 685–688.

Sirbescu, M.-L., Nabelek, P., 2003b. Crystallization conditions and evolution of magmatic fluids in the Harney Peak Granites and associated pegmatites, Black Hills, South Dakota – evidence from fluid inclusions. Geochem. Cosmochim. Acta 67, 2443–2465.

Smirnov, S.Z., 2015. The fluid regime of crystallization of water-saturated granitic and pegmatitic magmas: a physicochemical analysis. Russ. Geol. Geophys. 56 (9), 1292–1307.

Sowerby, J.R., Keppler, H., 2002. The effect of fluorine, boron, and excess sodium on the critical curve in the albite–H_2O system. Contrib. Mineral. Petrol. 143, 32–37.

Stilling, A., Černý, P., Vanstone, P.J., 2006. The Tanco pegmatite at Bernic Lake, Manitoba. XVI. Zonal and bulk compositions and their petrogenetic significance. Can. Mineral. 44, 599–623.

Stugard, Jr F., 1958. *Pegmatites of the Middletown area, Connecticut* (No. 1042-Q). US Govt. Print. Off.

Suwimonprecha, P., Cerny, P., Friedrich, G., 1995. Rare metal mineralization related to granites and pegmatites, Phuket, Thailand. Econ. Geol. 90 (3), 603–615.

Swanson, S.E., 2012. Mineralogy of spodumene pegmatites and related rocks in the tin–spodumene belt of North Carolina and South Carolina, USA. Can. Mineral. 50 (6), 1589–1608.

Swanson, S.E., Fenn, P.M., 1986. Quartz crystallization in igneous rocks. Am. Mineral. 71, 331–342.

Swanson, S.E., Fenn, P.M., 1992. The effect of F and Cl on the kinetics of albite crystallization: a model for granitic pegmatites? Can. Mineral. 30, 549-549.

Sweetapple, M.T., Collins, P.L., 2002. Genetic framework for the classification and distribution of Archean rare metal pegmatites in the North Pilbara Craton, Western Australia. Econ. Geol. 97 (4), 873–895.

Tang, Y., Wang, H., Zhang, H., Lv, Z.H., 2018. K-feldspar composition as an exploration tool for pegmatite-type rare metal deposits in Altay, NW China. J. Geochem. Explor. 185, 130–138.

Taylor, B.E., Foord, E.E., Friedrichsen, H., 1979. Stable isotope and fluid inclusion studies of gem-bearing granitic pegmatite-aplite dikes. San Diego Co., California. Contr. Mineral. and Petrol 68, 187–205.

Thomas, R., Davidson, P., 2007. The formation of granitic pegmatites from the viewpoint of melt and fluid inclusions and new experimental work. In: Granitic Pegmatites: the State of the Art – International Symposium. 06th – 12th May 2007, Porto, Portugal.

Thomas, R., Davidson, P., 2013. The missing link between granites and granitic pegmatites. J. Geosci. 58 (2), 183–200.

Thomas, R., Webster, J.D., Heinrich, W., 2000. Melt inclusions in pegmatite quartz: complete miscibility between silicate melts and hydrous fluids at low pressure. Contrib. Mineral. Petrol. 139 (4), 394–401.

Thomas, R., Förster, H.J., Heinrich, W., 2003. The behaviour of boron in a peraluminous granite-pegmatite system and associated hydrothermal solutions: a melt and fluid-inclusion study. Contrib. Mineral. Petrol. 144 (4), 457–472.

Thomas, R., Webster, J.D., Davidson, P., 2006. Understanding Pegmatite Formation: the Melt and Fluid Inclusion Approach, vol. 36. Book Chapter, Mineralogical Association of Canada Short Course, Montreal, Quebec, pp. 189–210.

Thomas, R., Davidson, P., Beurlen, H., 2011a. Tantalite- (Mn) from the Borborema Pegmatite Province, Northeastern Brazil: Conditions of Formation and Melt- and Fluid-Inclusion Constraints on Experimental Studies, pp. 749–759.

Thomas, R., Davidson, P., Schmidt, C., 2011b. Extreme alkali bicarbonate- and carbonate-rich fluid inclusions in granite pegmatites from the Precambrian Ronne granite, Bornholm Island, Denmark. Contrib. Mineral. Petrol. 161, 315–329.

Thomas, R., Davidson, P., Beurlen, H., 2012. The competing models for the origin and internal evolution of granitic pegmatites in the light of melt and fluid inclusion research. Mineral. Petrol. 106, 55–73.

Thomas, R., Davidson, P., Appel, K., 2019. The enhanced element enrichment in the supercritical states of granite–pegmatite systems. Acta Geochimica 38, 335–349.

Thoreau, J., 1950. La pegmatite stannifère de Manono, Katanga. CR de Travaux, CongrèsScientifique Elisabethville 41, 1–33.

Tindle, A.G., Breaks, F.W., Webb, P.C., 1998. Wodginite-group minerals from the Separation Rapids rare-element granitic pegmatite group, northwestern Ontario. Can. Mineral. 36 (2), 637–658.

Tkachev, A.V., 2011. Evolution of metallogeny of granitic pegmatites associated with orogens throughout geological time. Geological Society, London, Special Publications 350 (1), 7–23.

Tremblay, L.P., 1978. Uranium subprovinces and types of uranium deposits in the Precambrian rocks of Saskatchewan. Geological Survey of Canada. Pap. 78–1A, 427–435.

Troch, J., Huber, C., Bachmann, O., 2022. The physical and chemical evolution of magmatic fluids in near-solidus silicic magma reservoirs: implications for the formation of pegmatites. Am. Mineral. 107 (2), 190–205.

Trueman, D.L., Černý, P., 1982. Exploration for rare-element granitic pegmatites. In: Černý, P. (Ed.), Granitic Pegmatites in Science and Industry, vol. 8. Mineralogical Association of Canada Short Course Handbook, pp. 463–494.

Tyler, P.M., 1950. Economic Importance of Pegmatites, vol. 7550. United States Bureau of Mines.

Tyrrell, G.W., 1978. Composition and Constitution of Magmas. In the Principles of Petrology. Springer, Dordrecht, pp. 46–56.

Uher, P., Cerny, P., Chapman, R., Hatar, J., Miko, O., 1998. Evolution of Nb, Ta-oxide minerals in the Prasiva granitic pegmatites, Slovakia; II, External hydrothermal Pb, Sb overprint. Can. Mineral. 36 (2), 535–545.

Utsunomiya, A., Ota, T., Windley, B.F., Suzuki, N., Uchio, Y., Munekata, K., Maruyama, S., 2007. History of the Pacific superplume: implication for Pacific paleogeography since the late proterozoic. In: Yuen, D.A., Maruyama, S., Karato, S., Windley, B.F. (Eds.), Superplumes: beyond Plate Tectonics. Springer, Dordrecht, pp. 363–407.

Van Daele, J., Hulsbosch, N., Dewaele, S., Boiron, M.-C., Piessens, K., Boyce, A., Muchez, P., 2018. Mixing of magmatic-hydrothermal and metamorphic fluids and the origin of peribatholitic Sn vein-type deposits in Rwanda. Ore Geol. Rev. 101, 481–501.

Veksler, I.V., Thomas, R., 2002. An experimental study of B-, P-and F-rich synthetic granite pegmatite at 0.1 and 0.2 GPa. Contrib. Mineral. Petrol. 143 (6), 673–683.

Virk, H.S., Singh, S., 1977. Fission track dating and uranium mineralization in pegmatites of Bhilwara area, Rajasthan State (India). Mineral. J. 8 (5), 263–271.

Vlasov, K.A., 1952. Structure-paragenetic classification of granitic pegmatites. Izvestiya Akademii Nauk SSSR. Seriya Geologicheskaya 2, 30–55 (in Russian).

Vlasov, K.A., 1961. Principles of classifying of granite pegmatites and their textural-paragenetic types. Transactions of the Academy of Sciences, USSR, Geologic Series 1, 5–20.

Wang, Z., Li, J., Chen, Z., Yan, Q., Xiong, X., Li, P., Deng, J., 2021. Evolution and Li mineralization of the No. 134 pegmatite in the Jiajika rare-metal deposit, western Sichuan, China: constrains from critical minerals. Minerals 12 (1), 45.

Wang, J.M., Hou, K.S., Yang, L., Liu, X.C., Wang, R.C., Li, G.M., Fu, J.G., Hu, F.Y., Tian, Y.L., Wu, F.Y., 2023. Mineralogy, petrology and PT conditions of the spodumene pegmatites and surrounding meta-sediments in Lhozhag, eastern Himalaya. Lithos 456, 107295.

Webber, K.L., Simmons, Wm.B., 2007. Crystallization dynamics. In: Martins, T., Vieira, R. (Eds.), Granitic Pegmatites: the State of the Art, Book of Abstracts, Memórias N. 8, pp. 17–19. Porto, Portugal.

Webber, K.L., Falster, A.U., Simmons, W.B., Foord, E.E., 1997. The role of diffusion-controlled oscillatory nucleation in the formation of line rock in pegmatite-aplite dikes. J. Petrol. 38, 1777–1791.

Webber, K.L., Simmons, W.B., Falster, A.U., Foord, E.E., 1999. Cooling rates and crystallization dynamics of shallow level pegmatite-aplite dikes. San Diego County, California. American Mineralogists 84, 708–717.

Webber, K.L., Simmons, W.B., Falster, A.U., Hanson, S.L., 2019. Anatectic pegmatites of the Oxford County pegmatite field, Maine, USA. Can. Mineral. 57, 811–815.

Webber, K., Simmons, W.B., Falster, A.U., Roda-Robles, E., 2023. Pegmatite Formation by Direct Anatexis: Oxford County Pegmatite Field, Maine. Sudbury 2023 GAC-MAC SGA Abstract SS20.

Webster, J.D., Thomas, R., Rhede, D., Förster, H.J., Seltmann, R., 1997. Melt inclusions in quartz from an evolved peraluminous pegmatite: geochemical evidence for strong tin enrichment in fluorine-rich and phosphorus-rich residual liquids. Geochem. Cosmochim. Acta 61 (13), 2589–2604.

Webster, J., Thomas, R., Förster, H.J., Seltmann, R., Tappen, C., 2004. Geochemical evolution of halogen-enriched granite magmas and mineralizing fluids of the Zinnwald tin-tungsten mining district, Erzgebirge, Germany. Miner. Deposita 39 (4), 452–472.

Winkler, H.G.F., 1976. Petrogenesis of Metamorphic Rocks. Springer-Verlag, New York, p. 334.

Wise, M.A., 1999. Characterization and classification of NYF-type pegmatites. Can. Mineral. 37, 802–803.

Wise, M.A., Müller, A., Simmons, W.B., 2022. A proposed new mineralogical classification system for granitic pegmatites. Can. Mineral. 60 (2), 229–248.

Wu, M., Samson, I.M., Zhang, D., 2018. Textural features and chemical evolution in Ta-Nb oxides: implications for deuteric rare-metal mineralization in the Yichun granite-marginal pegmatite, southeastern China. Econ. Geol. 113 (4), 937–960.

Wu, B., Bonnetti, C., Liu, Y., Zhang, Z.S., Guo, G.L., Li, G.L., Hu, Y.Q., Yan, Z.Y., 2021. Uraninite from the guangshigou pegmatite-type uranium deposit in the north Qinling orogen, Central China: its occurrence, alteration and implications for post-Caledonian uranium circulation. Minerals 11, 729.

Xu, L., Chen, L., Zhao, J., Li, J., Wang, S., Yang, W., Li, J., Yang, B., Wang, H., Yang, Y., Zhang, Z., 2024. Magmatic-hydrothermal evolution of the Dangba rare-metal granitic pegmatites in the Songpan–Ganzê orogenic belt, Eastern Tibet: insights from muscovite and columbite-group minerals. J. Geochem. Explor. 265, 107559.

Yin, R., Huang, X.L., Xu, Y.G., Wang, R.C., Wang, H., Yuan, C., Ma, Q., Sun, X.M., Chen, L.L., 2020. Mineralogical constraints on the magmatic–hydrothermal evolution of rare-elements deposits in the Bailongshan granitic pegmatites, Xinjiang, NW China. Lithos 352, 105208.

Yuan, F., Liu, J., Carranza, E.J.M., Zhai, D., Wang, Y., Zhang, S., Sha, Y., Liu, G., Wu, J., 2018. The Guangshigou uranium deposit, northern Qinling Orogen, China: a product of assimilation-fractional crystallization of pegmatitic magma. Ore Geol. Rev. 99, 17–41.

Zagorsky, V.Y., Peretyazhko, I.S., Shmakin, B.M., 1999. Granitic Pegmatites, Miarolitic Pegmatites 3. Nauka, Novosibirsk, p. 485 (in Russian).

Zagorsky, V.Ye., Makagon, V.M., Shmakin, B.M., 2003. Systematics of granitic pegmatites. Russ. Geol. Geophys. 44, 422–435.

Zaw, K., 1998. Geological evolution of selected granitic pegmatites in Myanmar (Burma): constraints from regional setting, lithology, and fluid-inclusion studies. Int. Geol. Rev. 40 (7), 647–662.

Zhou, J., Zhang, H., Tang, Y., Lv, Z., Guan, S., 2023. Characteristics and geological significance of CO2-rich fluid inclusions in Dakalasu No. 1 pegmatite Dyke, Altay. Minerals 13 (3), 365.

Zhu, J., Zhu, W., Xu, Z., Zhang, R., Che, X., Zheng, B., 2023. The geochronology of pegmatites in the Jiajika lithium deposit, western Sichuan, China: implications for multi-stage magmatic-hydrothermal events in the Songpan-Ganze rare metal metallogenic belt. Ore Geol. Rev., 105582

Zimanovskaya, N.A., Oitseva, T.A., Khromykh, S.V., Travin, A.V., Bissatova, A.Y., Annikova, I.Y., Aitbayeva, S.S., 2022. Geology, mineralogy, and age of Li-bearing pegmatites: case study of tochka deposit (east Kazakhstan). Minerals 12 (12), 1478.

Zwaan, J.H., Seifert, A.V., Vrána, S., Laurs, B.M., Anckar, B., Simmons, W.B.S., Falster, A. U., Lustenhouwer, W.J., Muhlmeister, S., Koivula, J.I., Garcia-Guillerminet, H., 2005. Emeralds of the Kafubu area, Zambia. Gems Gemol. 41 (2), 116–148.